The chemistry of group 10 metal *triangulo* clusters [1]

Andrew D. Burrows, D. Michael P. Mingos *

Department of Chemistry, Imperial College of Science, Technology and Medicine, South Kensington, London SW7 2AY, UK

Contents

Abstract

For the group 10 metals, nickel, palladium and platinum, M$_3$ *triangulo* clusters display a wide chemistry which increases in scope on descending the triad. The substitution and addition

* Corresponding author.
[1] Dedicated to the memory of Joseph Chatt.

chemistry of these compounds is reviewed, focusing mainly on platinum but drawing on palladium and nickel when relevant comparisons and contrasts can be made. The synthesis of *triangulo* clusters from monomeric compounds and bonding theories are also reviewed. Substitution reactions of $[Pt_3(\mu\text{-}X)_3Y_3]$ clusters with CO, SO_2, isocyanides, phosphines, halides and NO^+ are discussed as are the addition and substitution reactions of $[Pt_3(\mu_3\text{-}CO)(\mu\text{-}dppm)_3]^{2+}$. Addition reactions of both types of *triangulo* clusters with metal fragments such as $Au(PR_3)^+$, M^+, Hg and metal halides are also discussed.

Keywords: Nickel; Palladium; Platinum; *Triangulo* clusters

List of abbreviations

Ac	acyl
Bu^n	*n*-butyl
Bu^t	*tert*-butyl
Bz	benzyl
COD	cyclooctadiene
Cp'	methylcyclopentadienyl
Cy	cyclohexyl
dba	dibenzylideneacetone
dmpm	bis(dimethylphosphino)methane
dmtc	dimethylthiocarbamate
dppm	bis(diphenylphosphino)methane
dppp	bis(diphenylphosphino)propane
Et	ethyl
Me	methyl
Ph	phenyl
PPN	bis(triphenylphosphoranylidene)ammonium
Pr^i	iso-propyl
R	alkyl or aryl
THF	tetrahydrofuran
Xyl	xylyl (2,6-dimethylphenyl)

1. Prologue

In 1965 one of us (D.M.P.M.) joined Professor Chatt's group at the University of Sussex having just graduated from UMIST. It was a new group at a new university, but fortunately there were some familiar faces around. Geoff Leigh had just resigned his lectureship at UMIST to join Chatt's Agricultural Research Council Unit of Nitrogen Fixation as a Scientific Officer and Mike Lappert had transferred from UMIST to Sussex University as a reader in the previous year. When I had first been interviewed by Chatt for a Ph.D. position a few months earlier he had talked about me continuing the C—H insertion reactions which he had discovered with

J.M. Davidson at the ICI Laboratories in Welwyn Garden City. When I arrived I think that it soon became apparent to him that there was an order of magnitude difference between my experimental skills and those of J.M. Davidson and he was forced to think of an easier project for me. Of course, the Chatt–Davidson work is now viewed as a classic piece of organometallic chemistry since it pioneered the whole area of C$-$H activation by transition metal compounds with low oxidation states. So the opportunity for me to make a contribution to what my subsequent colleague Malcolm Green was to describe as agostic interactions was lost forever. However, I still marvel at the way in which Davidson was able to handle such air-sensitive compounds at a time when the techniques for dealing with air-sensitive compounds were still relatively primitive.

It so happened that Paulo Chini was visiting the laboratories for a few months as a NATO Fellow prior to taking up a permanent appointment at the University of Milan. Since this visit was drawing towards a close Professor Chatt thought it an excellent opportunity for Paulo Chini to pass on some of his outstanding skills for making and crystallizing compounds to the new, inexperienced and impractical research student. Therefore, for approximately one month I worked with Paulo on the synthesis and crystallisation of platinum–carbonyl–phosphine cluster compounds. The first formative observations in this area had been made by Chatt and Booth at the ICI Laboratories, but it was Paulo Chini who was able to separate and crystallize the compounds for the first time. It was a wonderful opportunity to see the way in which he separated the compounds by successive Soxhlet extractions, and his ability to produce wonderfully crystalline compounds. At that time $^{31}P(^{1}H)$ nuclear magnetic resonance (NMR) studies were of little value and the only technique available was IR spectroscopy. I recall one occasion when I was discovered by Chatt trying to work out the predicted group theoretical bands for the bridging carbonyls in the platinum clusters. It must have stuck because I remember Jim Ibers relating to me years later that Chatt's reference on my behalf noted my wayward theoretical bent.

I was to return to explore the chemistry of platinum triangular clusters in Oxford when I was appointed to a lectureship there in 1976. Coincidentally another Chatt man who moved to Oxford, Luigi Venanzi, was to prove a friendly rival in this area. Therefore, I thought it fitting to review this area for this memorial issue to Joseph Chatt.

2. Introduction

In recent years a large number and almost perplexing variety of structures have been characterized for transition metal cluster compounds. Fortunately many of these structures can now be rationalized on the basis of theoretical studies and often they can be described as being built up of smaller, simpler components of which the most recurrent is the M_3 triangle [1,2]. For the group 10 metals, Ni, Pd and Pt, M_3 *triangulo* clusters do not just act as building blocks for larger cluster compounds, but in addition they display a wide chemistry which increases in scope on descending the triad [3]. The substitution and addition chemistry of these compounds is
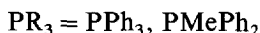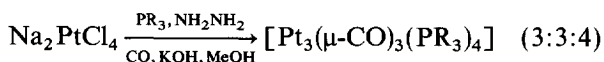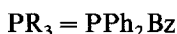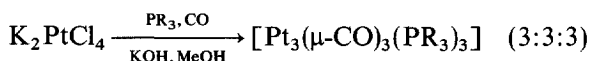
reviewed here and those reactions where the integrity of the M_3 triangle is retained are emphasized. The review will focus mainly on platinum chemistry for which research has been most extensive but will draw on palladium and nickel chemistry when appropriate comparisons and contrasts can be made. Prior to a discussion of the chemistry of these compounds the various synthetic procedures that have been employed to synthesize the *triangulo* clusters and some theoretical considerations are reviewed. Imhof and Venanzi have published a complementary review on the reactions of group 10 and 11 metal *triangulo* clusters with metal fragments [4].

3. Synthesis of *triangulo*-M_3 cluster compounds

Triangulo-platinum clusters can be synthesized either from Pt(II) compounds under reductive conditions or from Pt(0) monomers containing ligands which are readily displaced.

3.1. Reductive syntheses of triplatinum cluster compounds

The largest class of platinum *triangulo* clusters is the phosphine carbonyls which have the formula $[Pt_3(\mu\text{-}CO)_3(PR_3)_3]$ (often designated 3:3:3) or $[Pt_3(\mu\text{-}CO)_3(PR_3)_4]$ (3:3:4) [4]. These compounds were first observed from the carbonylation of alkyl platinum complexes [5] but the best early synthesis involved the reduction of alkali metal tetrachloroplatinates under CO in the presence of a phosphine ligand [6]:
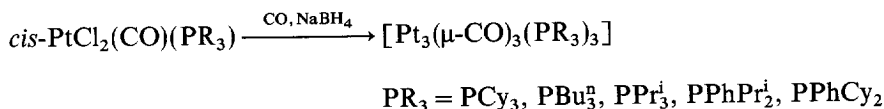
$$K_2PtCl_4 \xrightarrow[\text{KOH, MeOH}]{PR_3, CO} [Pt_3(\mu\text{-}CO)_3(PR_3)_3] \quad (3:3:3)$$

$$PR_3 = PPh_2Bz$$

$$Na_2PtCl_4 \xrightarrow[\text{CO, KOH, MeOH}]{PR_3, NH_2NH_2} [Pt_3(\mu\text{-}CO)_3(PR_3)_4] \quad (3:3:4)$$

$$PR_3 = PPh_3, PMePh_2$$

These reactions occur via the monomeric complex $[Pt(CO)_2(PR_3)_2]$. CO reduction of dihydrido complexes leads to good yields of the 3:3:3 complexes although this route is limited to complexes of bulky phosphines for which the dihydride is known [7,8]:

$$PtH_2(PR_3)_2 \xrightarrow{CO} [Pt_3(\mu\text{-}CO)_3(PR_3)_3]$$

$$PR_3 = PCy_3, PPr^i_3, PBu^t_3, PPh_2Bu^t$$
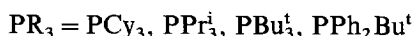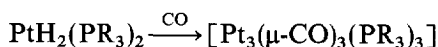
More general syntheses are based on the reduction of $[PtCl_2(CO)(PR_3)]$ complexes

by either sodium borohydride or zinc in the presence of CO [9,10]:

$$cis\text{-PtCl}_2(\text{CO})(\text{PR}_3) \xrightarrow{\text{CO, Zn}} [\text{Pt}_3(\mu\text{-CO})_3(\text{PR}_3)_3]$$

$$\text{PR}_3 = \text{PCy}_3, \text{P}(\text{CH}_2\text{CH}_2\text{CN})_3$$

$$cis\text{-PtCl}_2(\text{CO})(\text{PR}_3) \xrightarrow{\text{CO, NaBH}_4} [\text{Pt}_3(\mu\text{-CO})_3(\text{PR}_3)_3]$$

$$\text{PR}_3 = \text{PCy}_3, \text{PBu}^n_3, \text{PPr}^i_3, \text{PPhPr}^i_2, \text{PPhCy}_2$$
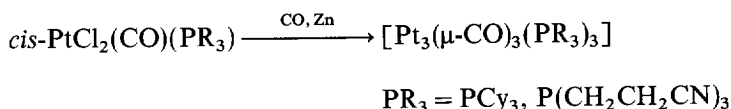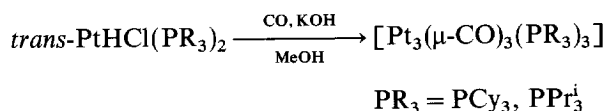
The nuclearity of the products from these reactions would appear to be dominated by the steric requirements of the phosphine ligands and the syntheses give rise to larger clusters when carried out with smaller phosphines, for example [10]

$$cis\text{-PtCl}_2(\text{CO})(\text{PMe}_2\text{Ph}) \xrightarrow{\text{CO, NaBH}_4} [\text{Pt}_4(\mu\text{-CO})_5(\text{PMe}_2\text{Ph})_4]$$
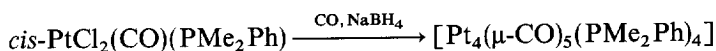
The zinc reduction is somewhat exceptional for PPh_3 as the product is a pentanuclear cluster, $[\text{Pt}_5(\mu\text{-CO})_5(\text{CO})(\text{PPh}_3)_4]$ [9]. Addition to the reaction mixture of a one-third equivalent of PPh_3 leads instead to the 3:3:4 cluster:
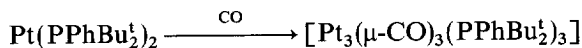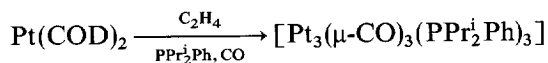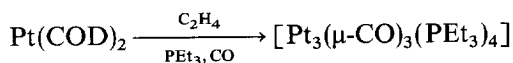
$$cis\text{-PtCl}_2(\text{CO})(\text{PPh}_3) \xrightarrow[\frac{1}{3}\text{eq. PPh}_3]{\text{CO, Zn}} [\text{Pt}_3(\mu\text{-CO})_3(\text{PPh}_3)_4]$$
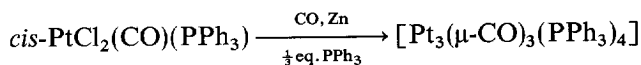
Reduction of $trans\text{-PtHCl}(\text{PR}_3)_2$ complexes also leads to cluster formation [11]:

$$trans\text{-PtHCl}(\text{PR}_3)_2 \xrightarrow[\text{MeOH}]{\text{CO, KOH}} [\text{Pt}_3(\mu\text{-CO})_3(\text{PR}_3)_3]$$

$$\text{PR}_3 = \text{PCy}_3, \text{PPr}^i_3$$

3.2. Syntheses from platinum(0) compounds

Triangulo clusters may also be synthesized from Pt(0) compounds and this provides the best synthetic route to *triangulo* clusters containing small phosphines such as PEt_3 [11–13]:
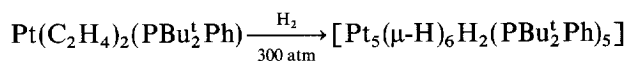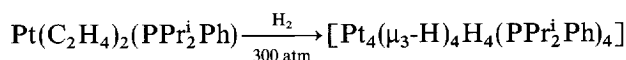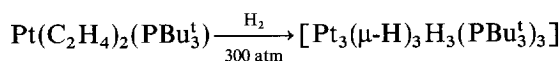
$$\text{Pt(COD)}_2 \xrightarrow[\text{PEt}_3, \text{CO}]{\text{C}_2\text{H}_4} [\text{Pt}_3(\mu\text{-CO})_3(\text{PEt}_3)_4]$$

$$\text{Pt(COD)}_2 \xrightarrow[\text{PPr}^i_2\text{Ph}, \text{CO}]{\text{C}_2\text{H}_4} [\text{Pt}_3(\mu\text{-CO})_3(\text{PPr}^i_2\text{Ph})_3]$$

$$\text{Pt(PPhBu}^t_2)_2 \xrightarrow{\text{CO}} [\text{Pt}_3(\mu\text{-CO})_3(\text{PPhBu}^t_2)_3]$$

$[\text{Pt(styrene)}_3]$ and $[\text{Pt}(\text{C}_2\text{H}_4)_2(\text{PR}_3)]$ have also been reported as precursors to 3:3:3 clusters [4].

In addition to determining the nuclearities of the clusters, the steric requirements of the phosphines appear to be the major factor in determining whether the syntheses

yield 42-electron 3:3:3 or 44-electron 3:3:4 carbonyl phosphine clusters. However, formation of stable 3:3:3 clusters with small phosphines such as $P(CH_2CH_2CN)_3$ and PBu_3^n suggests that the synthetic route might be important in determining what product is formed. PBu_3^n is a strong σ donor and poor π acceptor but $P(CH_2CH_2CN)_3$ is a poor σ donor resulting from the electron-withdrawing nature of the cyano groups.

The same general synthetic principles as illustrated above for carbonyl phosphine clusters can be applied to clusters containing other ligands. $[Pt(C_2H_4)_2(PR_3)]$ is a useful precursor to hydrido complexes. In this case the product nuclearity is critically dependent on the steric demands of the phosphine ligands [14,15]:
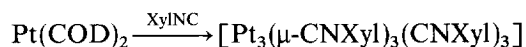
$$Pt(C_2H_4)_2(PBu_3^t) \xrightarrow[300\,atm]{H_2} [Pt_3(\mu\text{-}H)_3H_3(PBu_3^t)_3]$$

$$Pt(C_2H_4)_2(PPr_2^iPh) \xrightarrow[300\,atm]{H_2} [Pt_4(\mu_3\text{-}H)_4H_4(PPr_2^iPh)_4]$$

$$Pt(C_2H_4)_2(PBu_2^tPh) \xrightarrow[300\,atm]{H_2} [Pt_5(\mu\text{-}H)_6H_2(PBu_2^tPh)_5]$$

Similar precursors have been used to prepare SO_2-containing compounds [16], e.g.

$$Pt(C_2H_4)_2(PCy_3) \xrightarrow{SO_2} [Pt_3(\mu\text{-}SO_2)_3(PCy_3)_3]$$
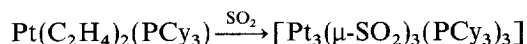
and $Pt(COD)_2$ has been used to prepare compounds containing bridging isocyanide and terminal phosphine ligands [17]:

$$Pt(COD)_2 \xrightarrow[PR_3]{XylNC} [Pt_3(\mu\text{-}CNXyl)_3(PR_3)_3]$$

$$PR_3 = PCy_3,\ PPh_3,\ PBz_3,\ PMe_2Ph,\ PMe_3$$
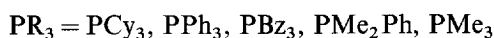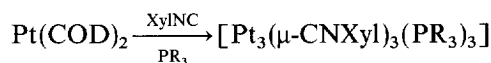
or bridging and terminal isocyanide ligands [18],

$$Pt(COD)_2 \xrightarrow{XylNC} [Pt_3(\mu\text{-}CNXyl)_3(CNXyl)_3]$$

All the above reactions have given rise to cluster compounds in which the oxidation state of platinum is zero. *Triangulo*-platinum clusters with higher oxidation states may also be prepared. The reaction of $Pt(O_2CCF_3)_2(dppm)$ with CO in aqueous acetone gives rise to a cluster compound [19] in which the metal atom oxidation state is formally $+\frac{2}{3}$:

$$Pt(O_2CCF_3)_2(dppm) \xrightarrow[acetone,\,H_2O]{CO,\,100\,^{\circ}C} [Pt_3(\mu_3\text{-}CO)(\mu\text{-}dppm)_3](CF_3CO_2)_2$$
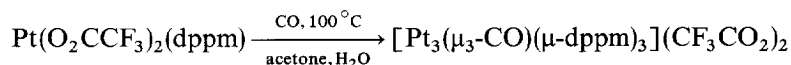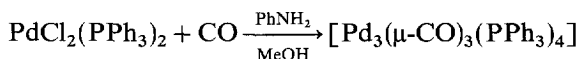
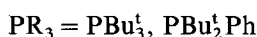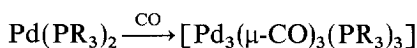## 3.3. Tripalladium cluster compounds

Palladium *triangulo* cluster compounds are somewhat less prevalent than their platinum analogues [20]. However, there are several examples of synthetic

routes to these clusters. $Pd(O_2CCF_3)_2(dppm)$ reacts in a similar manner to the platinum compound described above although in this case reaction occurs at room temperature [21].
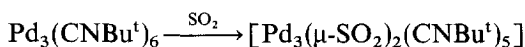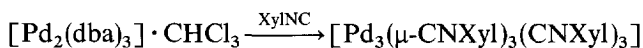
3:3:4 carbonyl phosphine clusters can be prepared from the reduction of palladium(II) compounds with various agents [22,23], for example

$$PdCl_2(PPh_3)_2 + CO \xrightarrow[\text{MeOH}]{\text{PhNH}_2} [Pd_3(\mu\text{-CO})_3(PPh_3)_4]$$

In an analogous manner to platinum chemistry 3:3:3 clusters can be prepared using bulky phosphine ligands from palladium(0) compounds and CO [13]:

$$Pd(PR_3)_2 \xrightarrow{\text{CO}} [Pd_3(\mu\text{-CO})_3(PR_3)_3]$$

$$PR_3 = PBu^t_3, PBu^t_2Ph$$

The Pd(0) species $[Pd_2(dba)_3] \cdot CHCl_3$ [24] and $Pd_3(CNBu^t)_6$ [25] both may be used to prepare *triangulo*-palladium compounds:

$$[Pd_2(dba)_3] \cdot CHCl_3 \xrightarrow{\text{XylNC}} [Pd_3(\mu\text{-CNXyl})_3(CNXyl)_3]$$

$$Pd_3(CNBu^t)_6 \xrightarrow{\text{SO}_2} [Pd_3(\mu\text{-SO}_2)_2(CNBu^t)_5]$$

Thermolysis techniques, although widely used in the cluster chemistry of osmium and other metals, have been less successful for the group 10 metals. One successful application has been the thermolysis of $[PdCl(PPh_3)_3]$ to give a *triangulo* cluster containing bridging PPh_2 ligands [26]:

$$PdCl(PPh_3)_3 \xrightarrow[\text{THF}]{125\,^\circ\text{C}} [Pd_3(\mu\text{-Cl})(\mu\text{-PPh}_2)_2(PPh_3)_3]^+$$
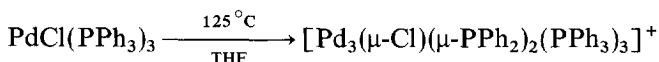
4. Bonding within *triangulo*-platinum cluster compounds

Transition metal complexes from groups 6 to 9 generally obey the 18-electron rule, and similarly cluster compounds of these metals obey the electron counting rules of the polyhedral skeletal electron pair theory [27]. The complexes and clusters of the later transition metals exhibit a greater flexibility in electron count as a result of large d–p promotion energies. Cluster compounds of the later transition metals are often characterized by fewer valence electrons that the clusters of earlier transition metals [28].

The structure of many platinum cluster compounds can be interpreted in terms of the bonding characteristics of the $Pt(PH_3)_2$ fragment. The bonding is dominated by the symmetries and energies of the skeletal molecular orbitals (MOs) formed from the $h_y(s$–$z)$ and $h_y(xy)$ frontier orbitals. These, in turn, depend markedly on the conformations adopted by the $Pt(PH_3)_2$ fragments [29].

For $Pt_3(PH_3)_6$ the calculations show that for a latitudinal arrangement there is a greater number of bonding and non-bonding orbitals than for a longitudinal arrangement. Hence, the more stable conformer would be expected to have a 42-electron latitudinal structure [29,30]:
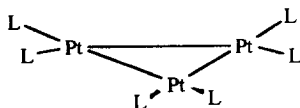
latitudinal arrangement,

42 bonding electrons
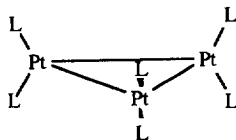
longitudinal arrangement,

40 bonding electrons

The frontier orbitals of the $Pt(PH_3)CO$ fragment are very similar to those for $Pt(PH_3)_2$, the major difference being the presence of low-lying π acceptor orbitals on the CO ligand. The MO scheme for $[Pt_3(CO)_3(PH_3)_3]$ is directly analogous to that for $[Pt_3(PH_3)_6]$ with the highest occupied MO (HOMO) of a′ symmetry and the lowest unoccupied MO (LUMO) a″ symmetry [31,32]. CO, unlike PH_3, has in-plane π^* orbitals and can bridge between two metal atoms. The μ-CO ligand can be treated as two 1-electron donors [33]. Frontier orbitals of the $Pt(CO)(PH_3)$ and angular $Pt(CO)_2(PH_3)$ fragments are very similar although there is a greater d character in the a_1 and b_2 frontier orbitals of the latter. Hence, on forming the cluster, direct metal–metal overlap is less in $[Pt_3(\mu$-CO$)_3(PH_3)_3]$ but this is more than compensated for by an increase in the overall metal–carbon overlap by virtue of the greater σ character. Overall, the bridging carbonyl geometry, $[Pt_3(\mu$-CO$)_3(PH_3)_3]$, is calculated to be 1.8 eV more stable than $[Pt_3(CO)_3(PH_3)_3]$ [32]. 42-electron carbonyl phosphine clusters all adopt this geometry with the platinum, phosphorus and carbonyl atoms essentially coplanar.

The MO diagram for $[Pt_3(\mu$-CO$)_3(PH_3)_3]$ is shown in Fig. 1. The HOMO is the $a_1′$ metal–metal bonding orbital. The two lowest unoccupied orbitals are the $a_2″$ bonding combination of metal p_z and CO π^* orbitals and an $a_2′$ antibonding combination of metal p_y orbitals although there is some d orbital contribution to this MO.

The relative energies of the unoccupied orbitals depend on the nature of the bridging and terminal ligands [34]. Both orbitals can be stabilized by bridging ligands that have low-lying orbitals of appropriate symmetry. Frontier orbitals for SO_2, CO, CNH and PH_2 are shown in Fig. 2. Both SO_2 and PH_2 have low-lying π^* acceptor orbitals which stabilize the $a_2′$ LUMO, which can be occupied in 44-electron clusters. The frontier orbital energy levels of 42-electron *triangulo*-platinum clusters with different bridging ligands are shown in Fig. 3.

Formation of 44-electron clusters by occupation of the $a_2′$ orbital leads to a lengthening of the Pt—Pt bonds as this orbital is metal–metal antibonding. Formation of a 44-electron cluster of the type $[Pt_3(\mu$-X$)_3Y_4]$ has less effect on the average Pt—Pt bond distance. However, in this case distortions in the triangle occur and the L_2Pt—PtL bonds are longer than the LPt—PtL bond.
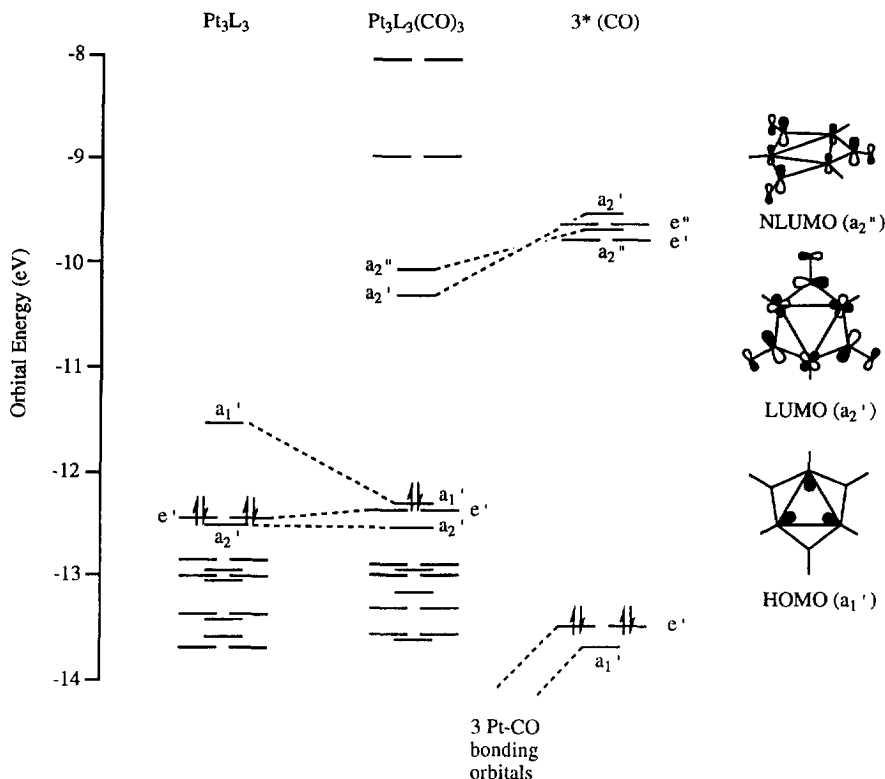
Fig. 1. MO diagram for $[Pt_3(\mu\text{-}CO)_3(PH_3)_3]$.

Pt—Pt bond distances for fifteen 42-electron *triangulo* clusters of the type $[Pt_3(\mu\text{-}X)_3(PR_3)_3]$ and nine 44-electron *triangulo* clusters of similar type are depicted graphically in Fig. 4. The results show, as expected, that 42-electron *triangulo* clusters generally have shorter Pt—Pt bond lengths than 44-electron clusters although the ranges overlap significantly. The 42-electron cluster $[Pt_3(\mu\text{-}SO_2)_3(PCy_3)_3]$ is somewhat exceptional having unusually large Pt—Pt bond distances owing to steric interactions between the SO_2 ligands and the cyclohexyl rings (see Section 5). Fig. 4 shows a larger spread of bond distances for the 44-electron compounds. The shorter Pt—Pt bonds are associated with compounds of the type $[Pt_3(\mu\text{-}X)_3(PR_3)_4]$ whereas the longer bonds are associated with compounds containing an extra electron pair in an a_2' orbital such as $[Pt_3(\mu\text{-}SO_2)_2(\mu\text{-}Br)(PCy_3)_3]^-$. Such observations are consistent with the MO considerations discussed above.

5. Carbonyl–sulphur dioxide exchange

Perhaps the most studied reaction of carbonyl phosphine clusters is the reaction with SO_2. The electronic properties of the SO_2 ligand are similar to those of the CO
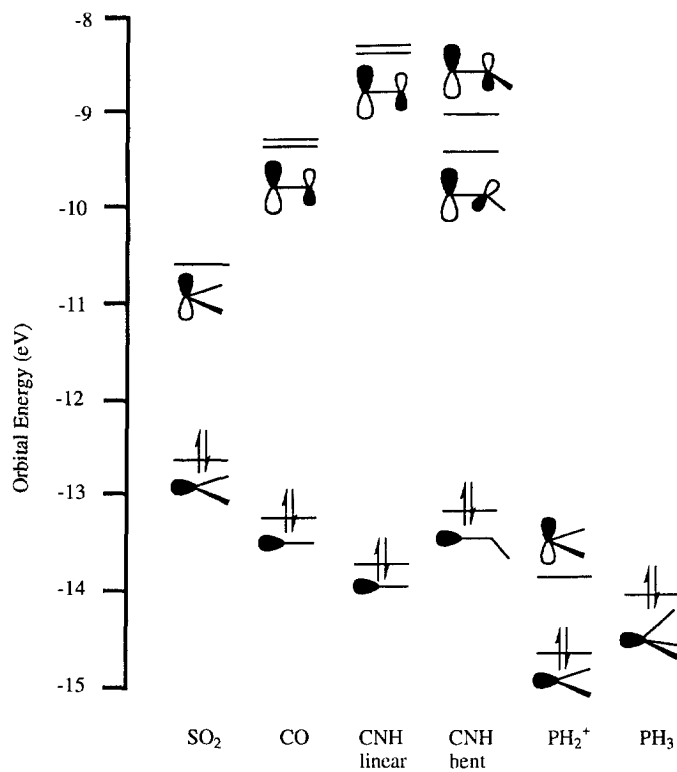
Fig. 2. Frontier orbitals for SO_2, CO, CNH and PH_2.
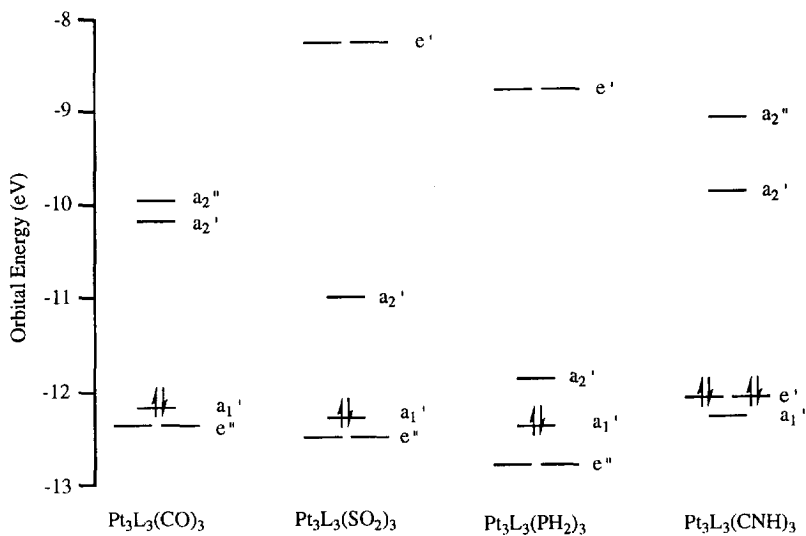
Fig. 3. Frontier orbital energy levels of the 42-electron clusters $[Pt_3(\mu\text{-}X)_3(PH_3)_3]$.
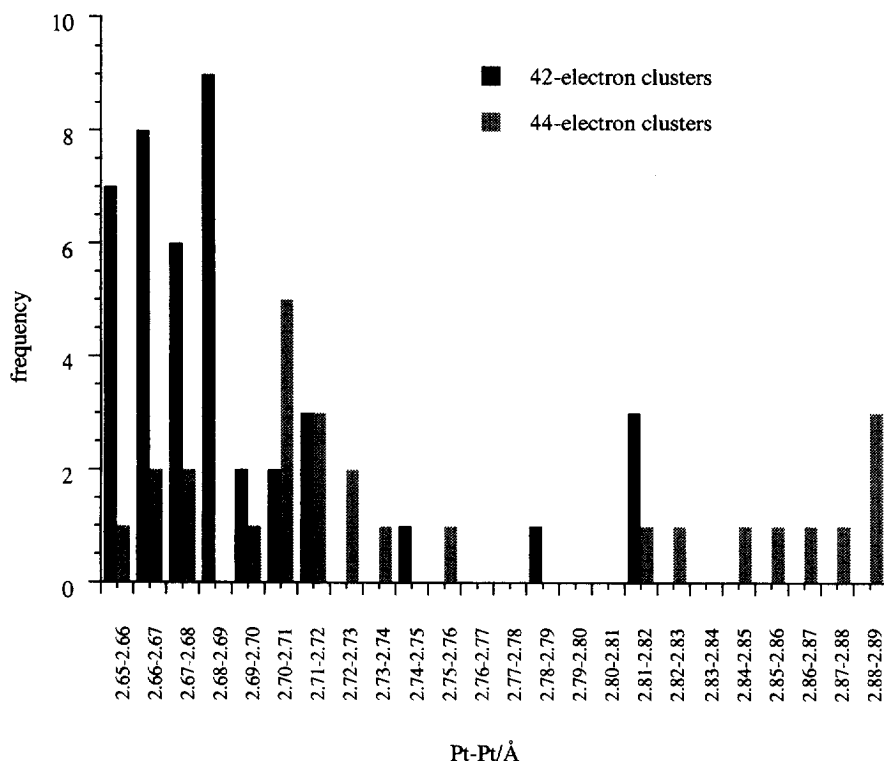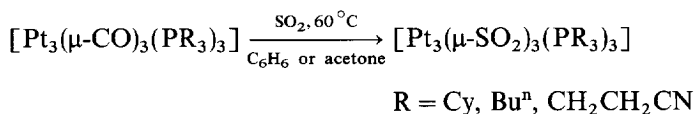
Fig. 4. Pt—Pt bond distances in 42- and 44-electrons *triangulo*-platinum clusters.

ligand although the former has a lower HOMO–LUMO gap which leads to stabilization of the a'_2 LUMO in the *triangulo* cluster [34]. A range of 3:3:3 clusters react with SO_2 at 60 °C leading to displacement of all carbonyls by bridging sulphur dioxide ligands [35]:

$$[Pt_3(\mu\text{-CO})_3(PR_3)_3] \xrightarrow[C_6H_6 \text{ or acetone}]{SO_2, 60 °C} [Pt_3(\mu\text{-SO}_2)_3(PR_3)_3]$$

$$R = Cy, Bu^n, CH_2CH_2CN$$

Similar products can also be obtained by degradation of tetraplatinum compounds [35], e.g.

$$[Pt_4(\mu\text{-CO})_5(PMe_2Ph)_4] \xrightarrow[C_6H_6]{SO_2, 60 °C} [Pt_3(\mu\text{-SO}_2)_3(PMe_2Ph)_3]$$
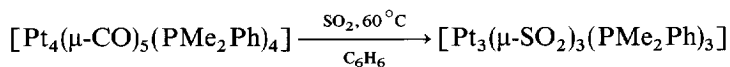
although the pentaplatinum cluster $[Pt_5(\mu\text{-CO})_5(CO)(PPh_3)_4]$ reacts with SO_2 to substitute three of the bridging CO ligands to give $[Pt_5(\mu\text{-CO})_2\text{-}(\mu\text{-SO}_2)_3(CO)(PPh_3)_4]$. The 3:3:4 cluster containing PPh_3 also reacts readily

with SO$_2$ [9,35]:

$$[Pt_3(\mu\text{-CO})_3(PPh_3)_4] \xrightarrow{SO_2} [Pt_3(\mu\text{-SO}_2)_3(PPh_3)_3]$$
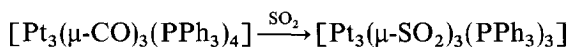
In this case a change in the electron count associated with the triangle, from 44 to 42, is observed. This probably has its origins in steric factors as the SO$_2$ ligands are more demanding than the CO ligands. Reaction of $[Pt_3(\mu\text{-SO}_2)_3(PPh_3)_3]$ with CO does not lead to the 42-electron species $[Pt_3(\mu\text{-CO})_3(PPh_3)_3]$ which has been shown to be electron deficient and unstable with respect to phosphine exchange [36], but to the pentanuclear cluster $[Pt_5(\mu\text{-CO})_5(CO)(PPh_3)_4]$. Sequential reaction with SO$_2$ and CO therefore represents a facile and high yielding conversion of $[Pt_3(\mu\text{-CO})_3(PPh_3)_4]$ to $[Pt_5(\mu\text{-CO})_5(CO)(PPh_3)_4]$. This transformation has also been observed on a number of column supports [37]. If the reaction is done in the presence of an additional one-third equivalent of phosphine, fragmentation of the *triangulo* cluster is suppressed and instead a mixed CO, SO$_2$ *triangulo* cluster is formed:

$$[Pt_3(\mu\text{-SO}_2)_3(PPh_3)_3] \xrightarrow{CO, \frac{1}{3}eq.\,PPh_3} [Pt_3(\mu\text{-CO})_2(\mu\text{-SO}_2)(PPh_3)_3]$$
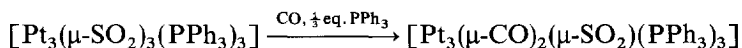
The PCy$_3$ system has been studied in some detail [38,39] and the observations are summarized in Scheme 1. Reactions with 1 equivalent of SO$_2$ or CO lead to
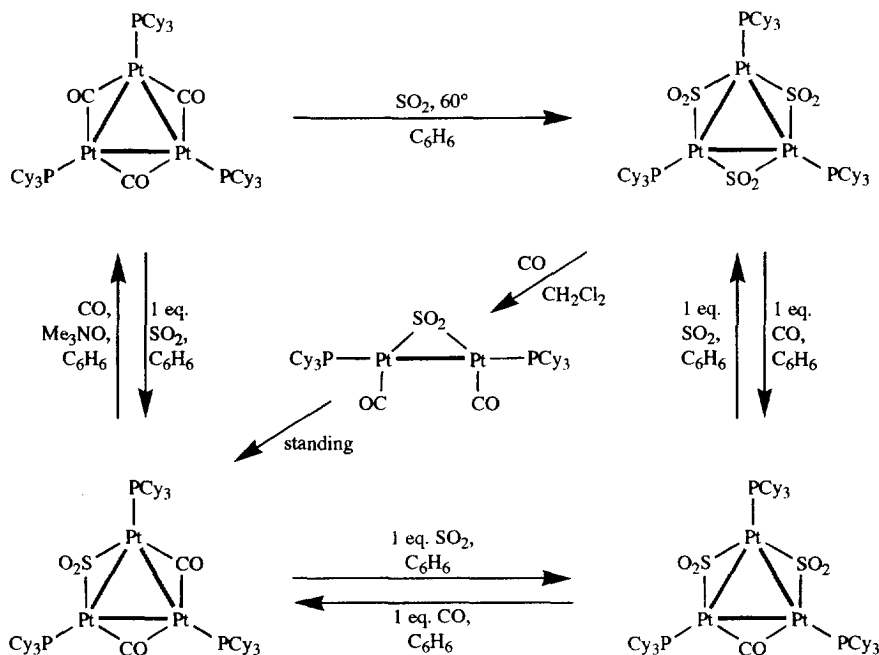
Scheme 1.

sequential replacement of CO by SO_2 or vice versa. The only exception to this is the conversion of $[Pt_3(\mu\text{-}CO)_2(\mu\text{-}SO_2)(PCy_3)_3]$ to $[Pt_3(\mu\text{-}CO)_3(PCy_3)_3]$ which requires excess CO and the presence of Me_3NO to facilitate the removal of the SO_2 ligand as Me_3NOSO_2. The rate of this reaction depends on the mole ratio of Me_3NO used. The dimer $[Pt_2(\mu\text{-}SO_2)(CO)_2(PCy_3)_2]$ was observed as an intermediate when the reaction of $[Pt_3(\mu\text{-}SO_2)_3(PCy_3)_3]$ with CO was carried out in dichloromethane. Stopped-flow IR studies have demonstrated that dimer formation in dichloromethane is very rapid, although no peaks due to monomeric species were observed.

The PBu_2^tPh system has also received considerable attention [40,41] and the results are summarized in Scheme 2. In contrast to the observations made for PCy_3, it is not possible to prepare the fully SO_2-substituted cluster nor is it possible to convert SO_2-substituted compounds back to $[Pt_3(\mu\text{-}CO)_3(PBu_2^tPh)_3]$ by reaction with CO. In addition, the dimeric species $[Pt_2(\mu\text{-}SO_2)(CO)_2(PBu_2^tPh)_2]$ can be readily isolated as the initial reaction product between $[Pt_3(\mu\text{-}CO)_3(PBu_2^tPh)_3]$ and SO_2. These differences between the two systems would appear to be a result of steric effects. Although PCy_3 and PBu_2^tPh have identical Tolman cone angles [42] ($170°$) this fails to take into account variations in conformational isomerism and ligand compression and meshing. Models evaluating non-bonding interactions between the phosphine ligands and cluster fragments have demonstrated that PBu_2^tPh is sterically more demanding that PCy_3 [41]. Hence reaction with SO_2 to form the partially substituted triangle occurs via a dimer. For the reaction of $[Pt_3(\mu\text{-}CO)_3(PCy_3)_3]$ with SO_2 a 44-electron intermediate has been postulated and indeed the crystal structure of $[Pt_3(\mu\text{-}CO)_3(PCy_3)_4]$ has been reported [43]. Formation of such an intermediate removes the necessity of dissociation to the dimer in order for
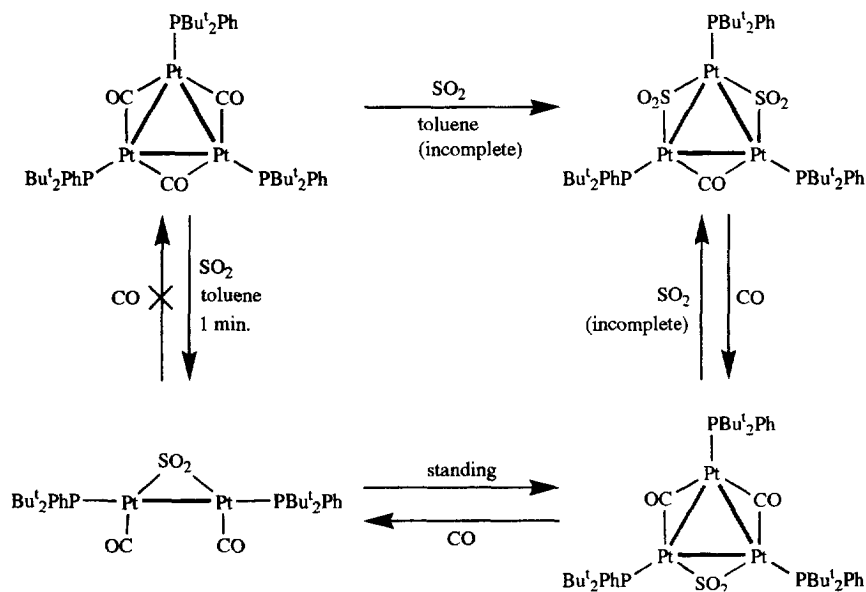
Scheme 2.

substitution to occur. However, the facile interconversion of dimers and *triangulo* clusters suggests that fragmentation and aggregation reactions are low energy processes. The sterically demanding nature of PBu^t_2Ph is also indicated in the crystal structure of $[Pt_3(\mu\text{-}CO)_3(PBu^t_2Ph)_3]$ in which the carbonyl ligands are bent out of the plane of the metal atoms (Fig. 5).

All partially or fully SO_2 substituted *triangulo* clusters with monodentate phosphine ligands contain 42 electrons. The cluster $[Pt_3(\mu\text{-}SO_2)_3(PCy_3)_2(dppp)]$ [44] which has 44-electrons has been prepared (see Section 7) indicating that the barrier to the formation of a 3:3:4 cluster may be overcome if a bidentate ligand is used. Table 1 shows a comparison of Pt—Pt bond lengths in CO- and SO_2-substituted *triangulo* clusters. The Pt—Pt bond distances in $[Pt_3(\mu\text{-}SO_2)_3(PCy_3)_3]$, shown in Fig. 6, are considerably longer than in $[Pt_3(\mu\text{-}CO)_3(PCy_3)_3]$ and this is believed to be mainly due to steric repulsion between the SO_2 ligands and the cyclohexyl rings which are arranged in an eclipsed manner. The Pt—Pt bond distances are much shorter in $[Pt_3(\mu\text{-}SO_2)_3(PPh_3)_3]$ where the SO_2–phosphine repulsion is reduced although they are still longer than in the carbonyl phosphine clusters illustrating that the $\mu\text{-}SO_2$ ligand is more sterically demanding than the $\mu\text{-}CO$ ligand. In the unsymmetrical triangle $[Pt_3(\mu\text{-}CO)(\mu\text{-}SO_2)_2(PCy_3)_3]$ the bonds bridged by SO_2 are longer than that bridged by CO. Repulsion between the SO_2 ligands and the cyclohexyl groups is reduced in this case by a small distortion of the phosphines towards the carbonyl group.

All the compounds in the $[Pt_3(\mu\text{-}CO)_n(\mu\text{-}SO_2)_{3-n}(PCy_3)_3]$ series and many other phosphine containing cluster compounds have been characterized by $^{31}P(^1H)$ NMR spectroscopy. This is a powerful technique in platinum cluster chemistry as the natural abundancy of the $I = \frac{1}{2}$ nucleus ^{195}Pt (33.7%) leads to observed spectra being composed of the superimposed spectra for the various isotopomers. Some comment has been made concerning the magnitude of $^1J(Pt—Pt)$ coupling constants obtained from $^{195}Pt(^1H)$ NMR. These tend to be higher across bonds bridged by CO (1300–1830 Hz) than across bonds bridged by SO_2 (250–700 Hz) [39]. In comparison the value of $^1J(Pt—Pt)$ for $[Pt_3(\mu\text{-}CNBu^t)_3(CNBu^t)_3]$ is 188 Hz [49]. The value of

Table 1
Pt—Pt bond distances for carbonyl and sulphur dioxide substituted *triangulo*-platinum clusters

|	Number of electrons	$d(Pt—Pt)$ (Å)	Ref.
$[Pt_3(\mu\text{-}CO)_3(PCy_3)_3]$	42	2.653(2), 2.656(2), 2.656(2)	[45]
$[Pt_3(\mu\text{-}CO)_3(PBu^t_2Ph)_3]$	42	2.671(1), 2.673(1), 2.677(1)	[41]
		2.673(1), 2.683(1), 2.684(1)	
$[Pt_3(\mu\text{-}CO)_3(PPh_3)_3]$	42	2.657, 2.665, 2.667	[46]
$[Pt_3(\mu\text{-}CO)_3(PPh_2Bz)_3]$	42	2.65 (average)	[47]
$[Pt_3(\mu\text{-}CO)_3(PCy_3)_4]$	44	2.675(1), 2.714(1), 2.736(1)	[43]
$[Pt_3(\mu\text{-}CO)(\mu\text{-}SO_2)_2(PCy_3)_3]$	42	2.678(1), 2.710(1), 2.710(1)	[39]
$[Pt_3(\mu\text{-}SO_2)_3(PCy_3)_3]$	42	2.813(1), 2.814(1), 2.815(1)	[38]
$[Pt_3(\mu\text{-}SO_2)_3(PPh_3)_3]$	42	2.695(1), 2.695(1), 2.712(1)	[48]
$[Pt_3(\mu\text{-}CO)_3(PCy_3)_2(dppp)]$	44	2.753(1), 2.811(1), 2.826(1)	[44]
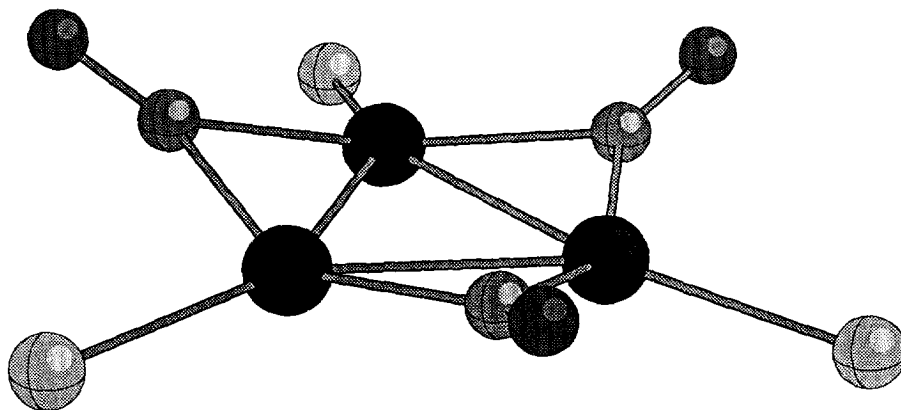
Fig. 5. Molecular structure of [Pt$_3$(μ-CO)$_3$(PBu$_2^t$Ph)$_3$], wtih *tert*-butyl and phenyl groups omitted for clarity, showing distortion of the carbonyl ligands from the metal plane.
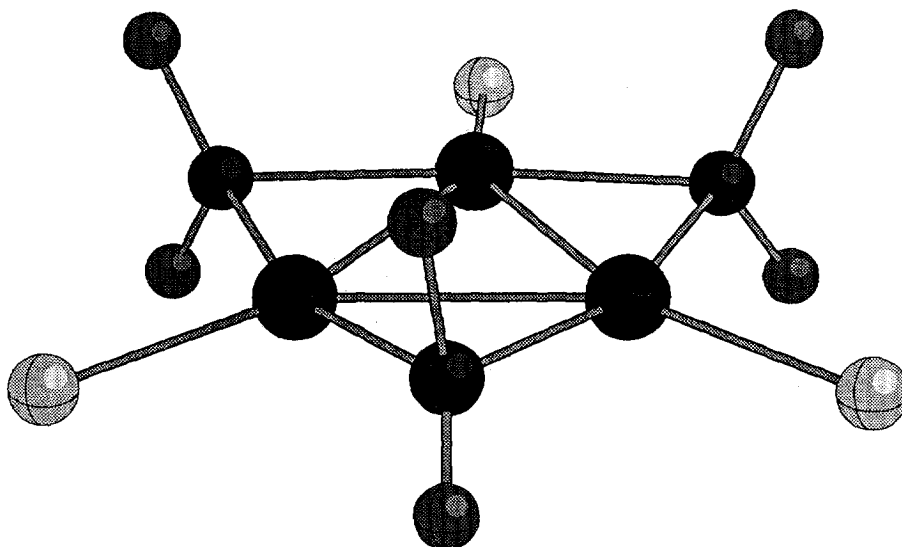
Fig. 6. Molecular structure of [Pt$_3$(μ-SO$_2$)$_3$(PCy$_3$)$_3$], with cyclohexyl groups omitted for clarity.

^1J(Pt—Pt) is related to the contribution of the Pt s orbitals to the metal–metal bonding which is presumably greatest for the CO-substituted case.

No simple rule would appear to relate any ^{31}P(^{1}H) NMR parameter to phosphine basicity though a correlation has been observed between v(CO) in [Pt$_3$(μ-CO)$_3$(PR$_3$)$_3$] and the phosphine basicity [41]. In addition, the IR frequencies for the series [Pt$_3$(μ-CO)$_n$(μ-SO$_2$)$_{3-n}$(PCy$_3$)$_3$] move to higher v(CO) and higher v(SO$_2$) as the proportion of SO$_2$ in the cluster increases (Table 2) [39]. This is consistent with SO$_2$ being a better π acceptor than CO.

Table 2
IR frequencies for the cluster compounds $[Pt_3(\mu\text{-}CO)_n(\mu\text{-}SO_2)_{3-n}(PCy_3)_3]$ $(n = 0\text{--}3)$

|	v(CO)	v(SO$_2$)
$[Pt_3(\mu\text{-}CO)_3(PCy_3)_3]$	1770 vs, 1737 w	—
$[Pt_3(\mu\text{-}CO)_2(\mu\text{-}SO_2)(PCy_3)_3]$	1847 m, 1784 vs	1206 w, 1070 s
$[Pt_3(\mu\text{-}CO)(\mu\text{-}SO_2)_2(PCy_3)_3]$	1840 vs	1234 m, 1080 s, 1071 vs
$[Pt_3(\mu\text{-}SO_2)_3(PCy_3)_3]$	—	1245 m, 1081 s

6. Reactions with isocyanides

The reactions in the Pt$_3$–CO–XylNC–PCy$_3$ system are summarized in Scheme 3 [17,50]. It is not possible to substitute from $[Pt_3(\mu\text{-}CO)_3(PCy_3)_3]$ either just the carbonyl ligands to give $[Pt_3(\mu\text{-}CNXyl)_3(PCy_3)_3]$ or all ligands to give $[Pt_3(\mu\text{-}CNXyl)_3(CNXyl)_3]$. Instead the products isolated from the reaction of $[Pt_3(\mu\text{-}CO)_3(PCy_3)_3]$ with XylNC have isocyanide substituted for either two CO ligands and one phosphine or all CO ligands and two phosphines. Crystal structures for both $[Pt_3(\mu\text{-}CO)(\mu\text{-}CNXyl)_2(CNXyl)(PCy_3)_2]$ and $[Pt_3(\mu\text{-}CNXyl)_3(CNXyl)_2(PCy_3)]$ show Pt—Pt bond distances within the usual range for 42-electron *triangulo*-platinum clusters with the bonds to Pt atoms bearing phosphine ligands somewhat longer than those bearing terminal isocyanide ligands. The crystal structures of these compounds show that the terminal isocyanide ligand is far less demanding sterically than PCy$_3$ but in contrast bridging isocyanide ligands, with C—N—C angles of around 130°, are sterically unfavourable across a Pt$_2$(PCy$_3$)$_2$ moiety. Hence the replacement of the first bridging carbonyl ligand by XylNC is accompanied by substitution of a terminal PCy$_3$ by XylNC, which in turn facilitates the replacement of a second bridging isocyanide. In a similar manner, the remaining carbonyl can only be replaced if an adjacent PCy$_3$ ligand is also lost making room for its bending distortion.

Despite these steric arguments it is possible to prepare $[Pt_3(\mu\text{-}CNXyl)_3(PCy_3)_3]$ not by substitution but directly from the reaction of Pt(COD)$_2$ with XylNC and PCy$_3$ [17]. The crystal structure of this compound has shown that the Pt—Pt bonds in this compound are shorter at an average of 2.68 Å than those in $[Pt_3(\mu\text{-}SO_2)_3(PCy_3)_3]$ [38] but slightly larger than those in $[Pt_3(\mu\text{-}CO)_3(PCy_3)_3]$. The shortening of the bonds with respect to $[Pt_3(\mu\text{-}SO_2)_3(PCy_3)_3]$ may in part be due to the smaller size of the bridging atom. There are certain distortions in the structure, shown in Fig. 7, to ease the expected steric crowding. The Pt—P bonds deviate from the plane defined by the metal triangle by an average of 10.4° and the bridging carbon atoms lie out of the metal plane in the opposite direction from the phosphines such that the average value of the dihedral angle between the metal plane and the Pt—C—Pt plane is 18.1°. In addition the average C—N—C angle for the isocyanide ligands is 140°, larger than reported for other platinum *triangulo* clusters with bridging isocyanides, and the phenyl rings deviate from the perpendicular by 34.7°.
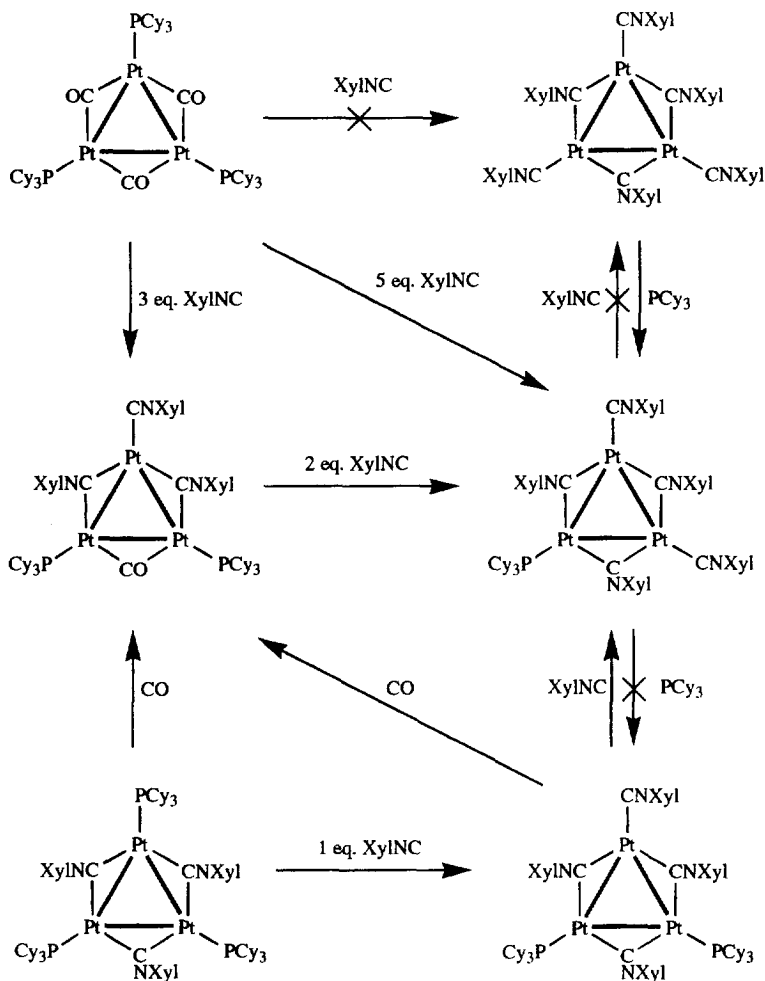
Scheme 3.

^1J(Pt,P) coupling constants [Pt$_3$(μ-CNXyl)$_3$(PR$_3$)$_3$] are comparable with those for [Pt$_3$(μ-CO)$_3$(PR$_3$)$_3$] but 400–900 Hz greater than for the analogous [Pt$_3$(μ-SO$_2$)$_3$(PR$_3$)$_3$] clusters. This coupling constant has been related to the s character of the Pt–P bond, which is affected by the electronic properties of the bridging ligands. It is possible that the weaker σ donor and better π acceptor properties of the SO$_2$ ligand relative to CNXyl reduce the s character of the Pt–P bond.

[Pt$_3$(μ-CNXyl)$_3$(PCy$_3$)$_3$] reacts with both XylNC and CO to give compounds containing a terminal isocyanide ligand (in the CO case via a rearrangement) and reduced steric crowding. The fact that several reactions yield [Pt$_3$(μ-CO)(μ-CNXyl)$_2$-(CNXyl)(PCy$_3$)$_2$] and [Pt$_3$(μ-CNXyl)$_3$(CNXyl)$_2$(PCy$_3$)] but they themselves do not undergo any substitution reactions suggests that these are the most stable
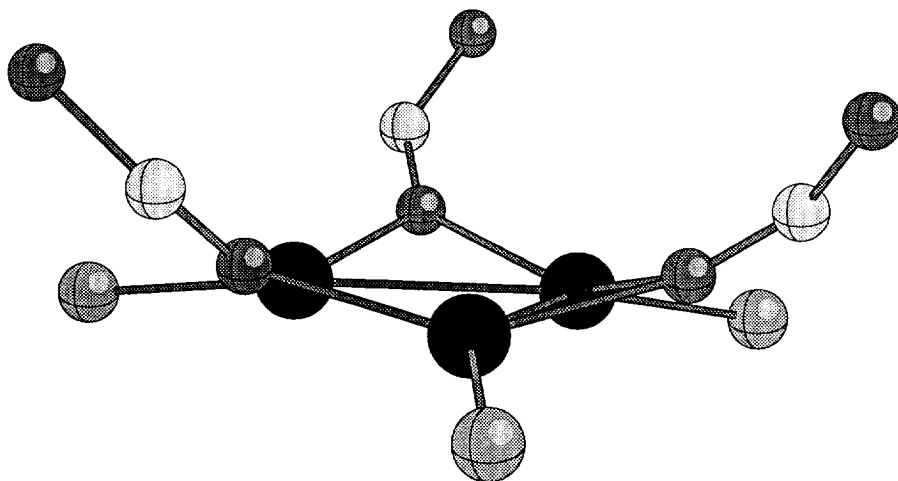
Fig. 7. Molecular structure of $[Pt_3(\mu\text{-}CNXyl)_3(PCy_3)_3]$, with xylyl and cyclohexyl groups omitted for clarity, showing distortions from planarity.

compounds in the system. They presumably represent the most effective compromise of the steric and electronic effects within the series. In general it appears that replacement of CO by XylNC is favourable electronically, but is limited by the steric constraints imposed by the bending requirement of the bridging isocyanide ligand.

In contrast to the reaction of $[Pt_3(\mu\text{-}CO)_3(PCy_3)_3]$, $[Pt_3(\mu\text{-}SO_2)_3(PCy_3)_3]$ reacts with two equivalents of XylNC to give a 44-electron *triangulo* cluster with terminal isocyanide ligands and with three equivalents of XylNC to give fragmentation to a dimer (Scheme 4) [51]. No substitution of the phosphine ligands occurs and no evidence has been observed for any intermediate or product containing bridging isocyanide. The SO_2 ligands appear to dominate the reaction pathway and even the mixed CO–SO_2 substituted clusters $[Pt_3(\mu\text{-}CO)_2(\mu\text{-}SO_2)(PCy_3)_3]$ and $[Pt_3(\mu\text{-}CO)(\mu\text{-}SO_2)_2(PCy_3)_3]$ react with XylNC to give the same products as $[Pt_3(\mu\text{-}SO_2)_3(PCy_3)_3]$ where stoichiometrically possible [39].

The Pt–P bond distances in $[Pt_3(\mu\text{-}SO_2)_2(CNXyl)_2(PCy_3)_3]$ are 2.7254(9), 2.7282(9) and 2.8422(9) Å, the longest being for the unbridged bond. These are within the usual range for 44-electron cluster compounds of platinum. Pt–Pt bond lengths are generally longer for 44-electron clusters than for 42-electron clusters as the additional electron pair lies in a MO that is somewhat antibonding with respect to the metal atoms.

The compound $[Pt_3(\mu\text{-}CNXyl)_3(CNXyl)_3]$ reacts with SO_2 but the product of the reaction is a pentanuclear cluster [52]:

$$[Pt_3(\mu\text{-}CNXyl)_3(CNXyl)_3] \xrightarrow{SO_2} [Pt_5(\mu\text{-}SO_2)_3(CNXyl)_7]$$
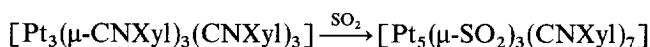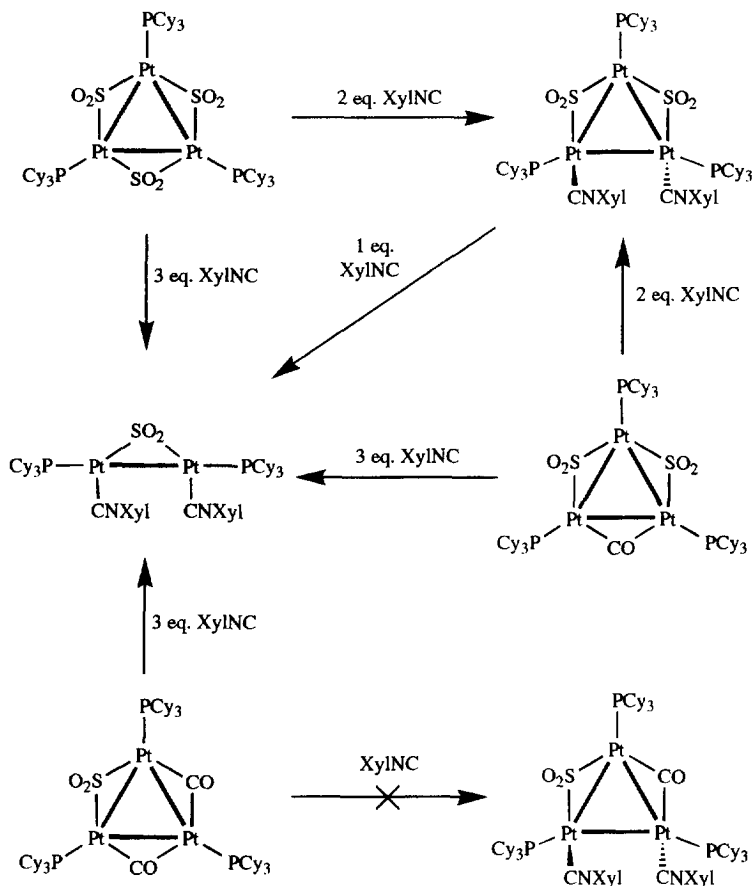
Scheme 4.

7. Reactions with phosphines

Generally, it is possible to substitute bulky phosphine ligands on *triangulo* clusters for other phosphines that are less sterically demanding [40]:

$$[Pt_3(\mu\text{-}CO)_3(PR_3)_3] \xrightarrow{PR'_3} [Pt_3(\mu\text{-}CO)_3(PR'_3)_3]$$

$$PR_3 = PBu^t_3 \qquad PR'_3 = PBu^t_2 Ph$$

$$PBu^t_2 Ph \qquad PBu^t Ph_2, PCy_3, PPr^i_3$$

$$PCy_3 \qquad PPr^i_3$$
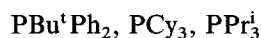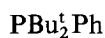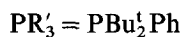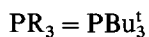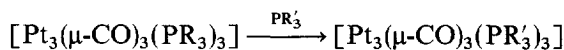
For the reaction of $[Pt_3(\mu\text{-}CO)_3(PBu^t_2 Ph)_3]$ and PCy_3 the intermediate $[Pt_3(\mu\text{-}CO)_3(PBu^t_2 Ph)_2(PCy_3)]$ can be isolated. In solution this slowly scrambles the phosphine ligands to give a mixture of $[Pt_3(\mu\text{-}CO)_3(PBu^t_2 Ph)_3]$,

$[Pt_3(\mu\text{-}CO)_3(PBu^t_2Ph)_2(PCy_3)]$ and $[Pt_3(\mu\text{-}CO)_3(PCy_3)_3]$. When an equimolar mixture of $[Pt_3(\mu\text{-}CO)_3(PBu^t_2Ph)_3]$ and $[Pt_3(\mu\text{-}^{13}CO)_3(PBu^t_2Ph)_3]$ is treated with 3 equivalents per Pt atom of PCy_3 the only products after 30 s are $[Pt_3(\mu\text{-}CO)_3(PCy_3)_3]$ and $[Pt_3(\mu\text{-}^{13}CO)_3(PCy_3)_3]$. This is only consistent with the platinum triangle remaining intact during the reaction. The reaction is believed to proceed through a 44-electron intermediate of the type $[Pt_3(\mu\text{-}CO)_3(PBu^t_2Ph)_3(PCy_3)]$. Although there is no direct evidence for this intermediate the circumstantial evidence is strong. $[Pt_3(\mu\text{-}CO)_3(PPh_2Bz)_3]$ reacts with an equivalent of PPh_2Bz to generate the 44-electron complex [12], i.e.

$$[Pt_3(\mu\text{-}CO)_3(PBz_3)_3] \xrightarrow{PBz_3} [Pt_3(\mu\text{-}CO)_3(PBz_3)_4]$$
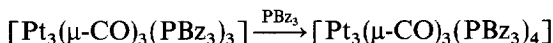
and the structure of $[Pt_3(\mu\text{-}CO)_3(PCy_3)_4]$ has been reported although this compound is not stable to phosphine loss in solution [43]. Clusters with bulky phosphines such as $[Pt_3(\mu\text{-}CO)_3(PBu^t_2Ph)_3]$ appear to be very stable with respect to fragmentation and addition of a large excess of phosphine gives no reaction. This is in contrast to $[Pt_3(\mu\text{-}CO)_3(PPh_3)_4]$ which immediately fragments to monomeric species under similar conditions [6].

In the structure of $[Pt_3(\mu\text{-}CO)_3(PCy_3)_4]$ the phosphorus atoms on the $Pt(PCy_3)$ fragments lie in the plane of the Pt_3 triangle whereas the phosphorus atoms on the $Pt(PCy_3)_2$ fragment lie in a plane perpendicular to the Pt_3 triangle [43]. A comparison of the Pt—Pt bond distances in $[Pt_3(\mu\text{-}CO)_3(PCy_3)_3]$ and $[Pt_3(\mu\text{-}CO)_3(PCy_3)_4]$ (Table 1) shows that the former is essentially equilateral whereas in the latter there is considerable distortion with the two bonds to the $Pt(PCy_3)_2$ fragments longer than that between the two $Pt(PCy_3)$ fragments. In addition, the carbonyl ligands are bound slightly more tightly to the $Pt(PCy_3)_2$ fragment. These observations are supported by overlap populations derived from molecular orbital calculations [34].

44-electron clusters can also be prepared by substitution of one phosphine ligand for a diphosphine (Scheme 5) [44]. This reaction even occurs with $[Pt_3(\mu\text{-}SO_2)_3(PCy_3)_3]$, in contrast to the reaction of $[Pt_3(\mu\text{-}CO)_3(PR_3)_4]$ with SO_2
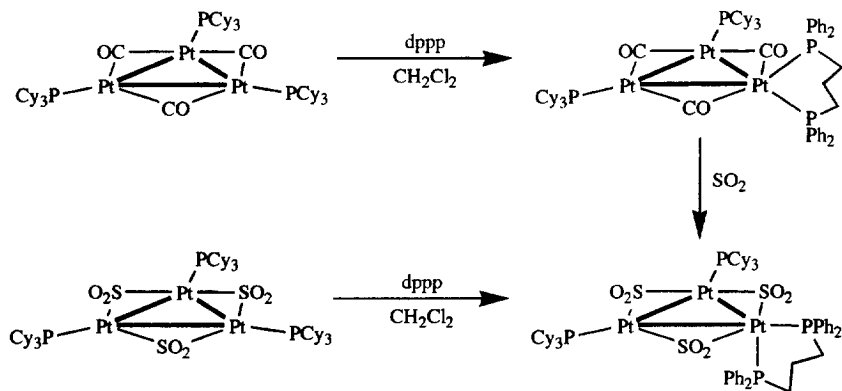
Scheme 5.

which only give 42-electron clusters as discussed above. There are important structural differences between the clusters $[Pt_3(\mu\text{-}CO)_3(PCy_3)_2(dppp)]$ and $[Pt_3(\mu\text{-}SO_2)_3(PCy_3)_2(dppp)]$. For the CO-substituted compound, $^{31}P(^1H)$ NMR spectroscopy shows that the two phosphorus atoms from the dppp ligand are equivalent, which is consistent with a structure in which the diphosphine bonds in a symmetrically chelating manner in a plane perpendicular to the Pt$_3$ triangle, in effect analogous to the structure of $[Pt_3(\mu\text{-}CO)_3(PCy_3)_4]$. In contrast, the $^{31}P(^1H)$ and $^{195}Pt(^1H)$ NMR spectra of the SO$_2$-substituted cluster are more complex with the dppp phosphorus atoms inequivalent. A crystal structure has shown that one of the phosphorus atoms is roughly in the Pt$_3$ plane whereas the other lies well below this plane. In addition, the SO$_2$ ligands are distorted out of the Pt$_3$ plane with the two bound to the platinum bearing the dppp distorted above the plane away from the diphosphine whereas the third is distorted below the plane (Fig. 8). The Pt—P bond length to the phosphorus atom below the plane is 2.376(7) Å which is considerably longer than the other Pt—P distances (average 2.28 Å). The P—Pt—P plane makes an angle of 66.1° with the metal plane. Consequently all four phosphorus atoms are in chemically distinct environments which is in agreement with the low temperature NMR data. Pt—Pt bond distances are 2.753(1), 2.811(1) and 2.826(1) Å with the lowest value representing the bond between the two Pt(PCy$_3$) fragments as expected.
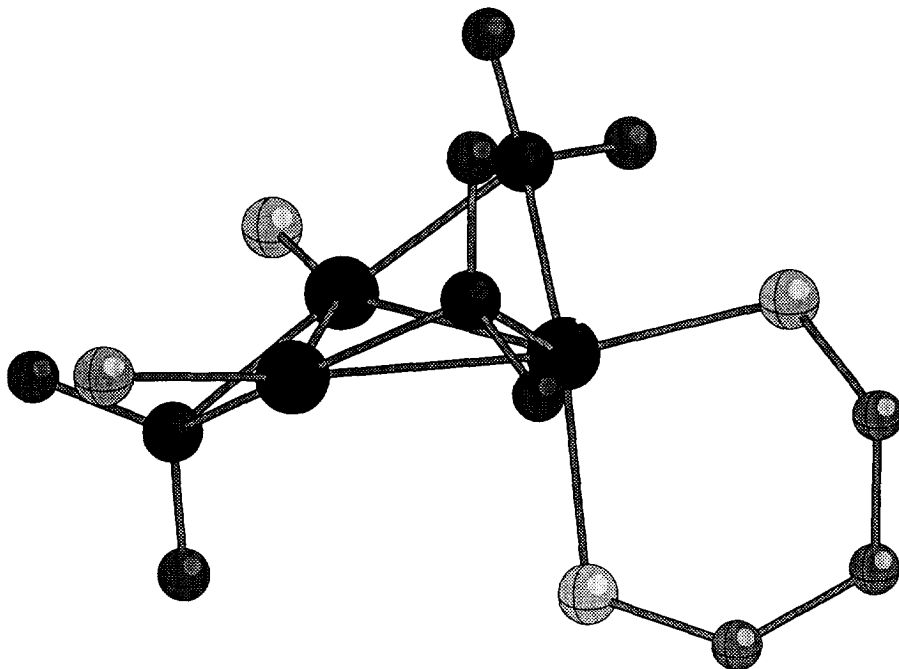

Fig. 8. Molecular structure of $[Pt_3(\mu\text{-}SO_2)_3(PCy_3)_2(dppp)]$, with phenyl and cyclohexyl groups omitted for clarity.

In these $[Pt_3(\mu\text{-}X)_3(PCy_3)_2(dppp)]$ clusters, two of the terminal ligands in $Pt_3(\mu\text{-}X)_3L_4$ are tied together, reducing the $P-Pt-P$ angle from $126°$ in $[Pt_3(\mu\text{-}CO)_3(PCy_3)_4]$ to $96.4°$ in $[Pt_3(\mu\text{-}SO_2)_3(PCy_3)_2(dppp)]$. Calculations have shown that $[Pt_3(\mu\text{-}SO_2)_3(PCy_3)_2(dppp)]$ would have a very small frontier orbital gap in the C_{2v} form, but distortion to the observed structure stabilizes the HOMO and opens up a significant HOMO–LUMO gap [34].

Similar reactions to those with dppp have been observed with the tri-phosphine ligand $MeC(CH_2PPh_2)_3$ [53]. Both 42-electron *triangulo* clusters $[Pt_3(\mu\text{-}X)_3(PCy_3)_3]$ ($X = CO$, SO_2) react to give 44-electron species of the formula $[Pt_3(\mu\text{-}X)_3(PCy_3)_2\{P,P'\text{-}(PPh_2CH_2)_2CMe(CH_2PPh_2)\}]$ ($X = CO$, SO_2) with the tri-phosphine bound by two phosphorus atoms and the third dangling. $^{31}P(^1H)$ NMR spectroscopy has shown that in both cases the observed product has the same symmetry as the analogous dppp compound.

Phosphine substitution reactions have also been observed in the palladium clusters of Dixon and co-workers with substitution of a phosphine ligand for one that is less demanding sterically [54]:

$$[Pd_3(\mu\text{-}Cl)(\mu\text{-}PPh_2)_2(PPh_3)_3]^+ \xrightarrow{PEt_3} [Pd_3(\mu\text{-}Cl)(\mu\text{-}PPh_2)_2(PEt_3)_3]^+$$
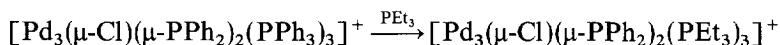
8. Reactions with halides

No reaction has been reported of a platinum carbonyl phosphine cluster with a halide. In contrast, the reaction of $[Pt_3(\mu\text{-}SO_2)_3(PR_3)_3]$ with halides occurs to give cluster compounds in which one SO_2 ligand has been replaced by a bridging halide. The reaction also occurs for the pseudohalide N_3^- [38].

Q = NEt$_3$Bz, X = Cl; Q = NEt$_4$, X = Br;
Q = PPN, X = N$_3$
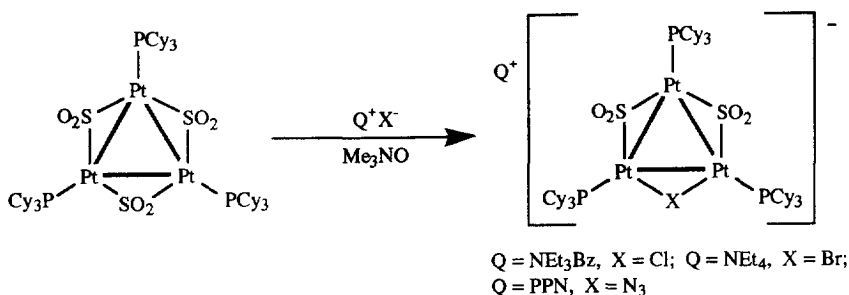
The rate of this reaction is strongly dependent on the size of the phosphine and the rate increases in the following series:

$$PCy_3 < PPh_3 < PMe_2Ph$$
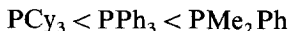
Indeed, for PCy_3 the reaction is still incomplete after 2 days. Reaction can be accelerated by the addition of Me_3NO, and with the use of this the reaction is complete after 15 min at room temperature. Reactions of the PMe_2Ph clusters were

complete after 10 min so it was not necessary to add Me_3NO. The strong steric effect of the phosphine on the rate of the reaction suggests that the reaction proceeds through a 44-electron "addition" intermediate, though there is no direct evidence for this. The reaction also occurs for the pseudohalide N_3^- although in this case the accelerating effect of Me_3NO was accompanied by the formation of byproducts. The crystal structure of the compound $NEt_4[Pt_3(\mu\text{-}SO_2)_2(\mu\text{-}Br)(PCy_3)_3]$ has been reported [38] but unfortunately the bridging ligands are disordered, and hence no meaningful comparison can be made of the individual Pt—Pt bond lengths. The average value is 2.886 Å, which is longer by 0.072 Å than in $[Pt_3(\mu\text{-}SO_2)_3(PCy_3)_3]$, the increase as expected with the additional electron pair residing in a molecular orbital with some metal–metal antibonding character.

The reason that the SO_2-substituted clusters react with halide in contrast to the CO-substituted clusters is that the LUMO (a_2') which becomes the HOMO of the 44-electron substituted cluster is lower in energy in the SO_2 case, owing to the increased π acid nature of the SO_2 ligand (see Section 4). Calculations give a significantly lower overlap population for the edge bridged by the 4-electron donor. The crystallographic disorder has prevented this from being verified from the crystal structure but it is consistent with the NMR coupling constant parameters. For example, in $NEt_4[Pt_3(\mu\text{-}SO_2)_2(\mu\text{-}Br)(PCy_3)_3]$ $^2J(Pt_2-P_1)$ (across SO_2) is 307 Hz whereas $^2J(Pt_1-P_1')$ (across Br) is 240 Hz.

9. Substitution reactions with $NOBF_4$

$[Pt_3(\mu\text{-}CO)_3(PCy_3)_3]$ reacts with an excess of $NOBF_4$ in benzene–methanol to give a nitrosyl-containing cluster [55]:
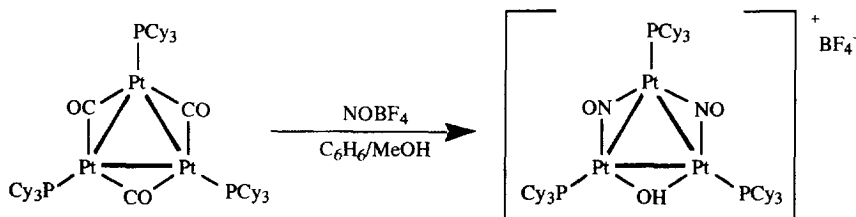
Pt—Pt bond distances are 2.736(1), 2.739(1) and 2.772(1) Å, within the expected range for 44-electron *triangulo* clusters. The hydrogen atom in the bridging hydroxyl groups was not located in the crystal structure although evidence for its presence was observed in the IR spectrum ($v(OH)$ at 3543 cm^{-1}), and the ^1H NMR spectrum (δ at 3.7 ppm (br)). The hydroxyl ligand is believed to originate from trace amounts of water present.

The anionic tripalladium cluster $[Pd_3(\mu\text{-}SO_2)_2(\mu\text{-}Cl)(PPh_3)_3]^-$ also reacts with $NOBF_4$, in this case to substitute one of the SO_2 ligands for NO^+:

$$\text{NEt}_3\text{Bz}^+ \quad \left[\begin{array}{c} \text{PPh}_3 \\ | \\ \text{Pd} \\ \text{O}_2\text{S} \diagup \quad \diagdown \text{SO}_2 \\ | \quad | \\ \text{Pd} \text{---} \text{Pd} \\ \text{Ph}_3\text{P} \diagup \quad \diagdown \text{Cl} \diagup \quad \diagdown \text{PPh}_3 \end{array}\right]^- \quad \xrightarrow{\text{NOBF}_4} \quad \begin{array}{c} \text{PPh}_3 \\ | \\ \text{Pd} \\ \text{O}_2\text{S} \diagup \quad \diagdown \text{NO} \\ | \quad | \\ \text{Pd} \text{---} \text{Pd} \\ \text{Ph}_3\text{P} \diagup \quad \diagdown \text{Cl} \diagup \quad \diagdown \text{PPh}_3 \end{array}$$
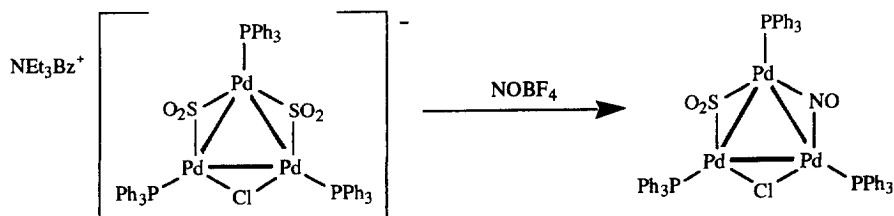
This leads to a neutral 44-electron *triangulo*-palladium cluster containing three different bridging ligands [56].

10. Substitution reactions of anionic *triangulo* clusters

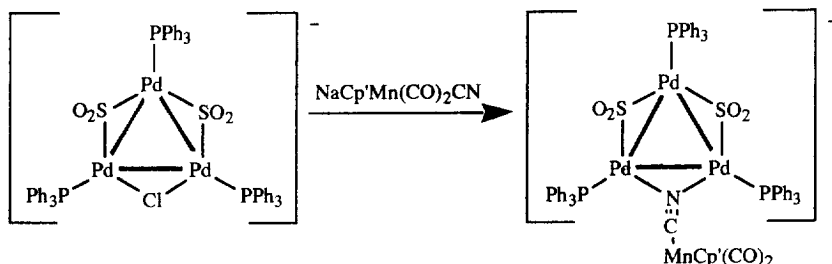Although no reactions of the clusters $[\text{Pt}_3(\mu\text{-SO}_2)_2(\mu\text{-Cl})(\text{PR}_3)_3]^-$ have been reported there are two series of chloride-bridged tripalladium clusters that have been studied. The palladium clusters $[\text{Pd}_3(\mu\text{-SO}_2)_2(\mu\text{-Cl})(\text{PPh}_3)_3]^-$ have been prepared from the reaction of $[\text{Pd}_5(\mu_3\text{-SO}_2)_2(\mu\text{-SO}_2)_2(\text{PPh}_3)_5]$ with chloride [56]. These compounds have been shown to substitute the chloride for either azide giving $[\text{Pd}_3(\mu\text{-SO}_2)_2(\mu\text{-N}_3)(\text{PPh}_3)_3]^-$ or for the cyanomanganate $[(\text{C}_5\text{H}_4\text{Me})\text{Mn}(\text{CO})_2\text{CN}]^-$ [57]:

$$\left[\begin{array}{c} \text{PPh}_3 \\ | \\ \text{Pd} \\ \text{O}_2\text{S} \diagup \quad \diagdown \text{SO}_2 \\ | \quad | \\ \text{Pd} \text{---} \text{Pd} \\ \text{Ph}_3\text{P} \diagup \quad \diagdown \text{Cl} \diagup \quad \diagdown \text{PPh}_3 \end{array}\right]^- \quad \xrightarrow{\text{NaCp'Mn(CO)}_2\text{CN}} \quad \left[\begin{array}{c} \text{PPh}_3 \\ | \\ \text{Pd} \\ \text{O}_2\text{S} \diagup \quad \diagdown \text{SO}_2 \\ | \quad | \\ \text{Pd} \text{---} \text{Pd} \\ \text{Ph}_3\text{P} \diagup \quad \diagdown \text{N} \diagup \quad \diagdown \text{PPh}_3 \\ \quad \| \\ \quad \text{C} \\ \quad | \\ \text{MnCp'(CO)}_2 \end{array}\right]^-$$

The cluster compounds $[\text{Pd}_3(\mu\text{-PPh}_2)_2(\mu\text{-Cl})(\text{PR}_3)_3]\text{BF}_4$ have been prepared by Dixon and co-workers and their substitution chemistry has been investigated in some detail [54,58,59]. The inert nature of the bridging PPh_2 groups directs all substitution reactions to the chloride, in contrast to the SO_2 containing systems. The reactions observed are detailed in Scheme 6. In the reaction with PHPh_2 the *p*-toluidine is added to scavenge the HCl formed in the reaction.

11. Reactions of the clusters $[\text{M}_3(\mu_3\text{-CO})(\mu\text{-dppm})_3]^{2+}$

So far the review has concentrated on the substitution reactions of clusters of the general formulae $[\text{M}_3(\mu\text{-X})_3\text{Y}_3]$ and $[\text{M}_3(\mu\text{-X})_3\text{Y}_4]$. The other major class of cluster compound for platinum and palladium has as its archetype $[\text{M}_3(\mu_3\text{-CO})(\mu\text{-dppm})_3]^{2+}$ and these compounds have received considerable study
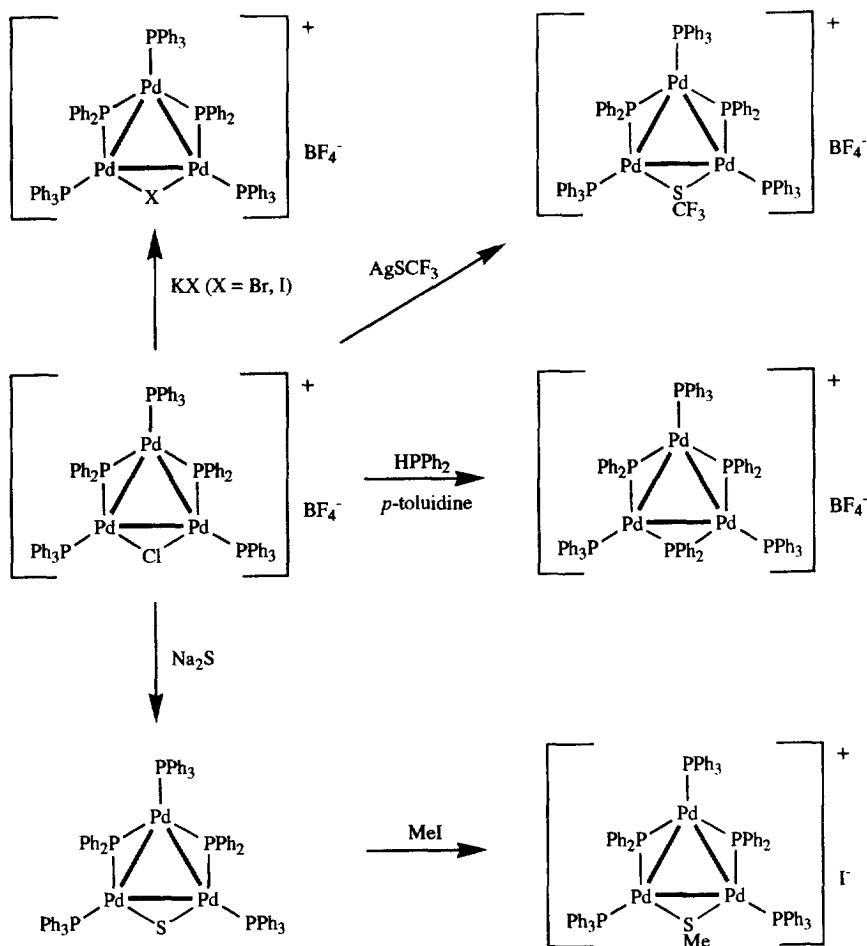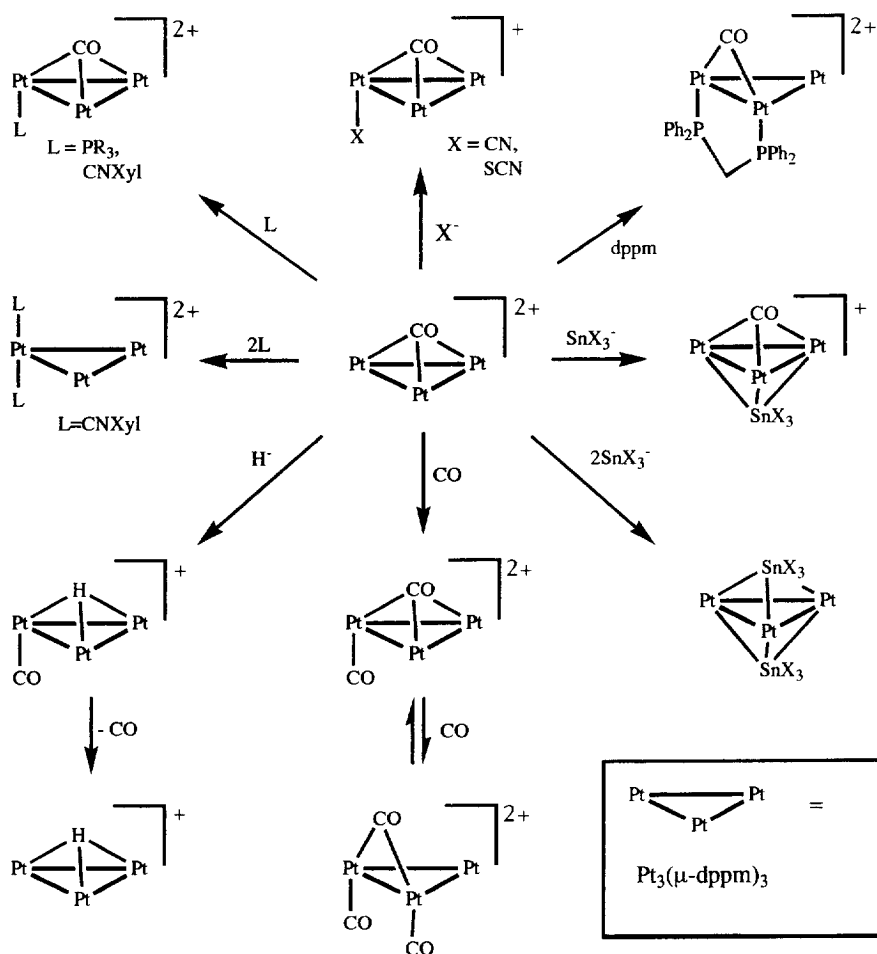
Scheme 6.

mainly from Puddephatt and co-workers. The chemistry has been described in a recent review [60] so only the main details are summarized here. The compounds $[M_3(\mu_3\text{-CO})(\mu\text{-dppm})_3]^{2+}$ contain 42 electrons as do clusters of the type $[M_3(\mu\text{-X})_3Y_3]$. The major difference is that these clusters are coordinatively unsaturated and readily undergo addition reactions as well as substitution reactions. The reactions of the more widely studied platinum clusters are given in Scheme 7 [60,61] and those of the palladium clusters in Scheme 8 [60–63].

Constrained by the bridging dppm ligands, the Pt–Pt bond distances do not show the same variations on increasing the electron count as do those in the $[M_3(\mu\text{-X})_3Y_3]$ clusters. This is also a result of the additional ligands using the empty p_z orbitals on the metal atoms rather than the empty metal–metal σ^* orbitals of the cluster. However, in the cluster $[Pt_3(CNXyl)_2(\mu\text{-dppm})_3]^{2+}$ [64] which is unusual
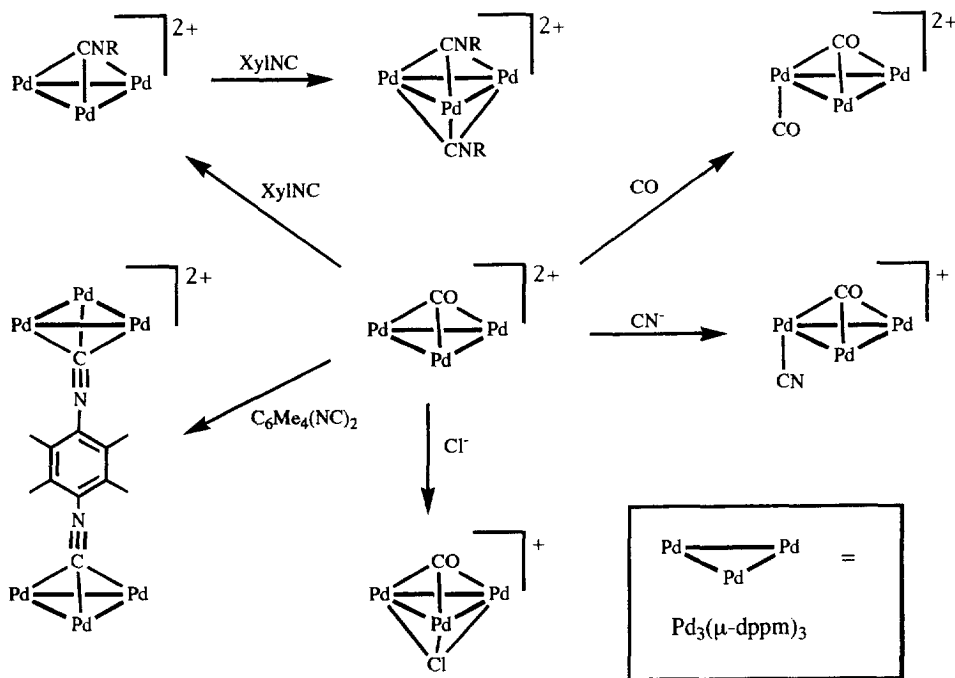
Scheme 7.

as it contains no atoms bridging between two or more metals there is a significant distortion, with both Pt—Pt bonds to the Pt atom bearing the two terminal isocyanide ligands being considerably longer at 2.6350(10) and 2.6515(9) Å than the bond between the two Pt atoms bound only to the phosphines, 2.5646(10) Å.

The electron count of clusters based on the $Pt_3(\mu\text{-dppm})_3$ moiety is not limited to 44, which is the largest number observed for a $[M_3(\mu\text{-X})_3Y_3]$ cluster. 44-electron clusters do occur (e.g. $[Pt_3(\mu_3\text{-CO})\{P(OPh)_3\}(\mu\text{-dppm})_3]^{2+}$ [65]) but so too do 46-electron clusters (e.g. $[Pt_3(\mu_3\text{-CO})(\mu\text{-dmpm})(\mu\text{-dppm})_3]^{2+}$ [66]), and some argument has even been made for clusters such as $[Pd_3(\mu_3\text{-CO})(\mu_3\text{-Cl})(\mu\text{-dppm})_3]^+$ containing 48 electrons, with the chloride ion contributing 6 electrons [32,62].

There are four structures of 44-electron clusters with the general formula $[Pt_3(\mu_3\text{-CO})L(\mu\text{-dppm})_3]^{n+}$ ($n = 1, 2$). Of these, one has L as a triply bridging ligand,

Scheme 8.

μ_3-SnF$_3$, while the other three contain terminal ligands, P(OPh)$_3$, SCN$^-$ and CN$^-$. The compound [Pt$_3(\mu_3$-CO)(μ_3-SnF$_3$)(μ-dppm)$_3$]$^+$ has crystallographically imposed threefold symmetry. The other three compounds all show a similar asymmetry of the bridging carbonyl ligand. In all cases the Pt—C bond to the Pt atom bearing the terminal ligand is shorter than those to the other two Pt atoms (Table 3). This can be rationalized as the carbonyl ligand is a π acceptor and will consequently bind preferentially to the most electron-rich platinum centre. The degree of slippage of the carbonyl from the symmetrical μ_3 bonding mode reflects the donor ability of

Table 3
Pt—C bond distances in carbonyl containing Pt$_3(\mu$-dppm)$_3$ clusters

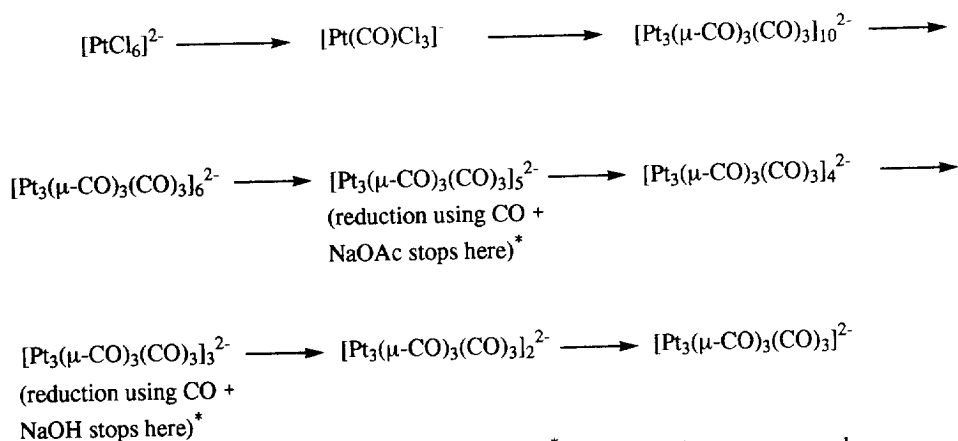|	Number of electrons	Pt–C bond distance (Å)	Ref.
[Pt$_3(\mu_3$-CO)(μ-dppm)$_3$]$^{2+}$	42	2.080(9), 2.089(8), 2.095(9)	[19]
[Pt$_3(\mu_3$-CO)(μ_3-SnF$_3$)(μ-dppm)$_3$]$^+$	44	2.16(5), 2.16(5), 2.16(5)	[67]
[Pt$_3(\mu_3$-CO){P(OPh)$_3$}(μ-dppm)$_3$]$^{2+}$	44	1.93(3), 2.16(3), 2.27(3)	[65]
[Pt$_3(\mu_3$-CO)(CN)(μ-dppm)$_3$]$^+$	44	1.94(2), 2.25(2), 2.44(2)	[61]
[Pt$_3(\mu_3$-CO)(SCN)(μ-dppm)$_3$]$^+$	44	2.04(2), 2.17(2), 2.18(2)	[68]
[Pt$_3(\mu$-CO)(μ-dmpm)$_4$]$^{2+}$	46	2.049(8), 2.061(9), 2.425(8)	[66]
[Pt$_3(\mu$-CO)(μ-dmtc)(μ-dppm)$_3$]$^+$	46	2.01(1), 2.02(1), 2.67(1)	[69]

the terminal ligand and it is greater for P(OPh)$_3$ than for SCN$^-$. This type of distortion is even greater in the 46-electron clusters $[Pt_3(\mu\text{-CO})(\mu\text{-dmpm})_4]^{2+}$ and $[Pt_3(\mu\text{-CO})(\mu\text{-dmtc})(\mu\text{-dppm})_3]^+$. Now there are two electron-rich platinum centres and the carbonyl binds in a μ_2 fashion between these atoms.
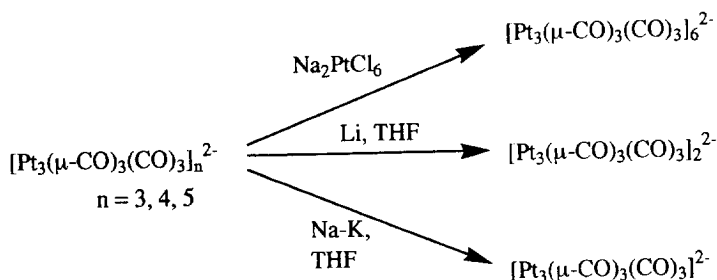
There are interesting differences in the chemistries of the related platinum and palladium clusters and one example of this is the reaction with isocyanides. $[Pt_3(\mu_3\text{-CO})(\mu\text{-dppm})_3]^{2+}$ reacts with one equivalent of XylNC to give an addition product with the isocyanide ligand terminally bound, $[Pt_3(\mu_3\text{-CO})(\text{CNXyl})\text{-}(\mu\text{-dppm})_3]^{2+}$. This then reacts with a further equivalent of isocyanide which substitutes the carbonyl ligand giving the compound $[Pt_3(\text{CNXyl})_2(\mu\text{-dppm})_3]^{2+}$ [64]. In contrast, $[Pd_3(\mu_3\text{-CO})(\mu\text{-dppm})_3]^{2+}$ reacts with one equivalent giving the substitution product $[Pd_3(\mu_3\text{-CNXyl})(\mu\text{-dppm})_3]^{2+}$ and reversibly with a further equivalent to give $[Pd_3(\mu_3\text{-CNXyl})_2(\mu\text{-dppm})_3]^{2+}$. No mixed carbonyl–isocyanide clusters were observed even in the presence of excess CO [63].

12. $[Pt_3(\mu\text{-CO})_3(CO)_3]_n^{2-}$ clusters

The series of clusters $[Pt_3(\mu\text{-CO})_3(CO)_3]_n^{2-}$ clusters ($n = 1$–6, 10) can be synthesized from the reduction of $[PtCl_6]^{2-}$ or $[Pt(CO)_2Cl_2]$ under CO [47,70] (Scheme 9). The product isolated depends critically on the nature and the quantity of the reducing agent used. The structures of these compounds for $n = 2$–5 show that they are based on stacking of $Pt_3(\mu\text{-CO})_3(CO)_3$ *triangulo* units, in all cases with the Pt$_3$ units close to, but not completely, eclipsed to generate D_{3h} symmetry. For $[Pt_3(\mu\text{-CO})_3(CO)_3]_2^{2-}$ (Fig. 9) there is a small translational distortion of the two *triangulo* fragments by 0.51 Å along one of the triangular Pt—Pt edges and a tilting of both the terminal and bridging carbonyl ligands in an outward direction from the Pt$_3$ plane. For $[Pt_3(\mu\text{-CO})_3(CO)_3]_3^{2-}$ the three Pt$_3$ triangular fragments are distorted from the idealized D_{3h} geometry primarily by a helical twisting of each Pt$_3$ unit relative to the adjacent unit of around 13°. The distortions in $[Pt_3(\mu\text{-CO})_3(CO)_3]_5^{2-}$ are more complex and illustrated in Fig. 10. There are large helical twistings between the second and third (27.2°) and third and fourth (28.6°) layers, and much smaller twisting between the first and second layers (8.1°), whereas the fourth and fifth layers are almost eclipsed (within 0.2°). These distortions from a regular prismatic stacking appear to represent a compromise between steric effects, repulsions between carbonyls in adjacent layers, and electronic effects, calculations of which have shown that the trigonal eclipsed geometry is favoured. Such calculations [71] on the interactions of anionic $[Pt_3(\mu\text{-CO})_3(CO)_3]^{2-}$ and neutral $[Pt_3(\mu\text{-CO})_3(CO)_3]$ fragments show that the a_2'' orbital of $[Pt_3(\mu\text{-CO})_3(CO)_3]^{2-}$ is directed out of plane, and the in-phase combination of this orbital for the two fragments stabilizes this combination (a_1') by about 0.3 eV in the dimer with respect to the a_2'' orbital of the monomer. Further addition of neutral monomer units causes the HOMO, always the in-phase combination derived from the a_2'' orbital in the monomer, to decrease in energy. Indeed, the insoluble species Pt(CO)$_2$ is now believed to have a polymeric structure based on stacked *triangulo* units, i.e. $[Pt_3(\mu\text{-CO})_3(CO)_3]_\infty^{2-}$, with hydronium ions incorporated to preserve overall neutrality.

$[PtCl_6]^{2-}$ ⟶ $[Pt(CO)Cl_3]^-$ ⟶ $[Pt_3(\mu\text{-}CO)_3(CO)_3]_{10}^{2-}$ ⟶

$[Pt_3(\mu\text{-}CO)_3(CO)_3]_6^{2-}$ ⟶ $[Pt_3(\mu\text{-}CO)_3(CO)_3]_5^{2-}$ ⟶ $[Pt_3(\mu\text{-}CO)_3(CO)_3]_4^{2-}$ ⟶
(reduction using CO +
NaOAc stops here)*

$[Pt_3(\mu\text{-}CO)_3(CO)_3]_3^{2-}$ ⟶ $[Pt_3(\mu\text{-}CO)_3(CO)_3]_2^{2-}$ ⟶ $[Pt_3(\mu\text{-}CO)_3(CO)_3]^{2-}$
(reduction using CO +
NaOH stops here)*

* unless very large excess used

Scheme 9.

Such oligomerization of Pt_3 fragments is only favourable for the anionic species and the linear approach of two neutral fragments has been shown to be repulsive.

^{195}Pt NMR spectroscopy has shown [72] that there is free rotation of the Pt_3 triangles around the C_3 axis and that in solution the triangles are exchanged between chains. Chemically, these stacked *triangulo* clusters may undergo reactions in which the number of Pt_3 units is either increased or decreased [70], for example

$$[Pt_3(\mu\text{-}CO)_3(CO)_3]_4^{2-} + [Pt_3(\mu\text{-}CO)_3(CO)_3]_2^{2-} \rightarrow 2[Pt_3(\mu\text{-}CO)_3(CO)_3]_3^{2-}$$
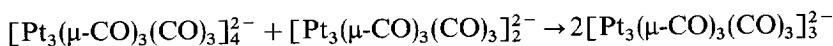
No palladium analogues to these clusters have been reported although the nickel cluster $[Ni(\mu\text{-}CO)_3(CO)_3]_2^{2-}$ has been shown, in contrast to $[Pt(\mu\text{-}CO)_3(CO)_3]_2^{2-}$, to have a trigonal antiprismatic arrangement of nickel atoms [73].

13. Reactions with electrophilic gold compounds

A number of 42-electron *triangulo* platinum clusters react with $[Au(PR_3)Cl]$ in the presence of $TlPF_6$ to generate 54-electron platinum–gold clusters (Schemes 10
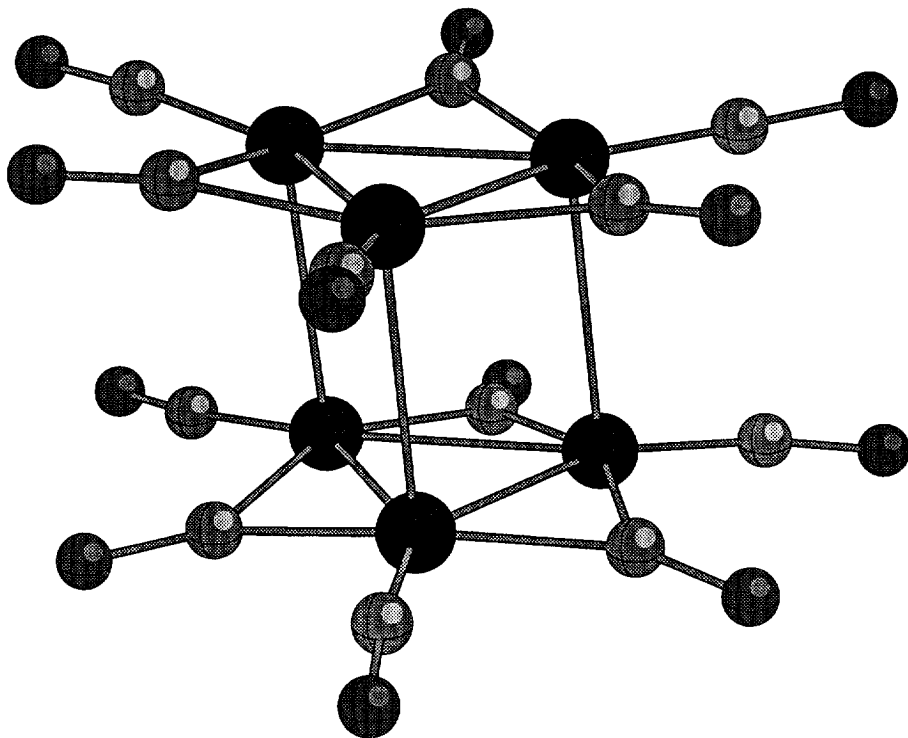
Fig. 9. Molecular structure of the anion in $(PPh_4)_2[Pt_3(\mu\text{-}CO)_3(CO)_3]_2$.

[74–76] and 11 [77,78]). In all these compounds the platinum atoms, phosphines and bridging ligands remain essentially coplanar. There is no bridging to the incoming gold atom which is said to be "capping" the triangle (Fig. 11). $[Pt_3(\mu\text{-}SO_2)_3(PCy_3)_3]$ reacts with $[Au\{P(C_6H_4F\text{-}p)_3\}Cl]$ without the presence of $TlPF_6$ to give a 56-electron platinum–gold cluster in which one SO_2 ligand has been substituted by chloride in addition to the capping of the triangle by the gold phosphine fragment [75]. This cluster reacts with a further equivalent of $[Au\{P(C_6H_4F\text{-}p)_3\}Cl]$ in the presence of $TlPF_6$ to give a 68-electron bicapped Pt_3Au_2 cluster compound [76], shown in Fig. 12. Platinum–platinum and platinum–gold bond distances for gold-capped platinum clusters are summarized in Table 4.

As can be seen from Table 4 no increase is observed in the Pt—Au bond lengths on moving from a 54- to a 56-electron cluster, although this change in electron count does lead to an increase in the Pt—Pt bond distances. Calculations show that the additional electron pair resides in an a_2' orbital which is localized primarily on the platinum triangle, the $Au(PR_3)$ fragment having no frontier orbitals of a_2 symmetry. Since this a_2' orbital is platinum–platinum antibonding its occupation leads to the observed lengthening of the Pt—Pt bonds [79].

In the cluster $[\{(C_6H_4F\text{-}p)_3PAu\}_2Pt_3(\mu\text{-}SO_2)_2(\mu\text{-}Cl)(PCy_3)_3]^+$ the platinum–platinum and gold–platinum bond distances are somewhat longer than in the Pt_3Au

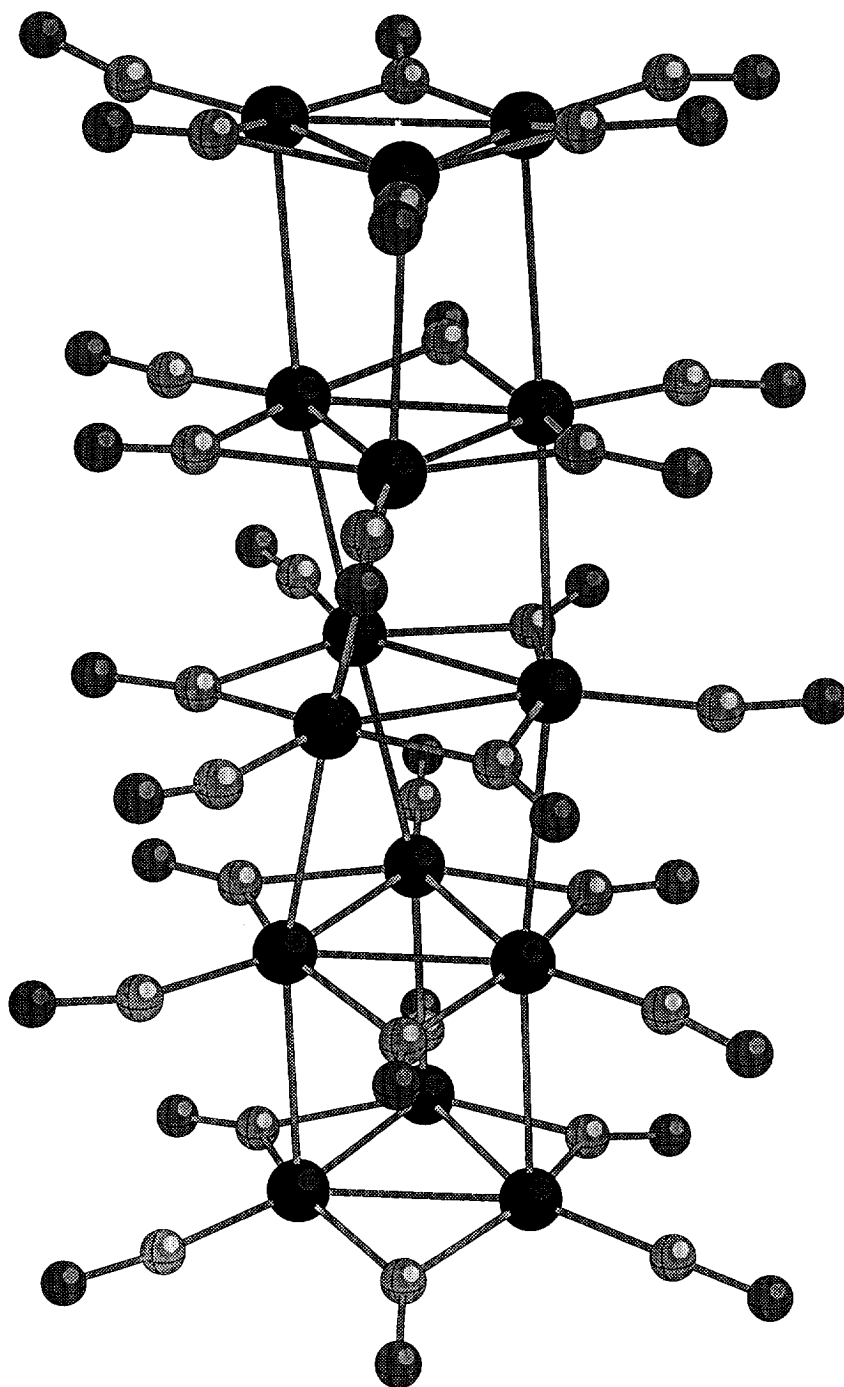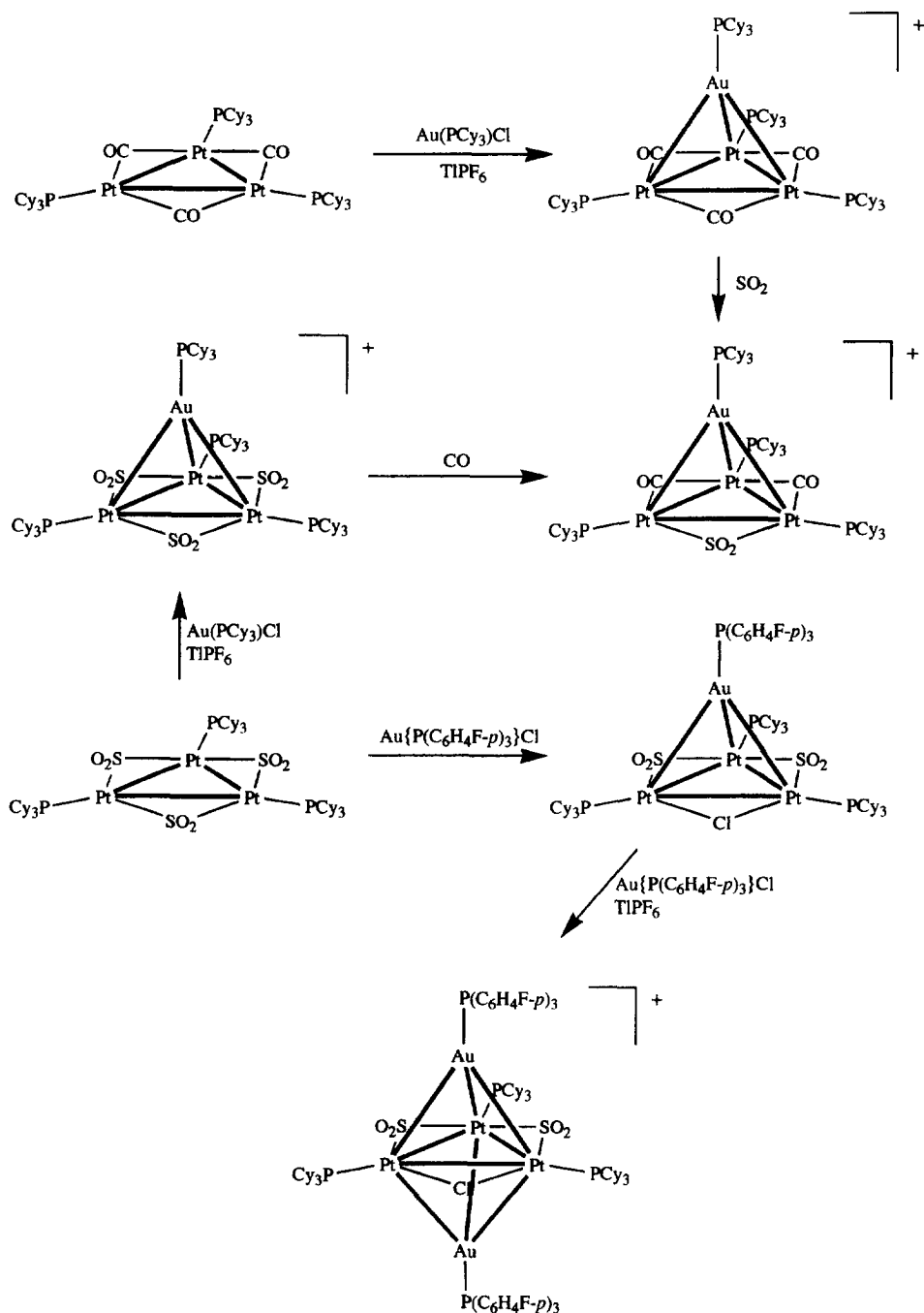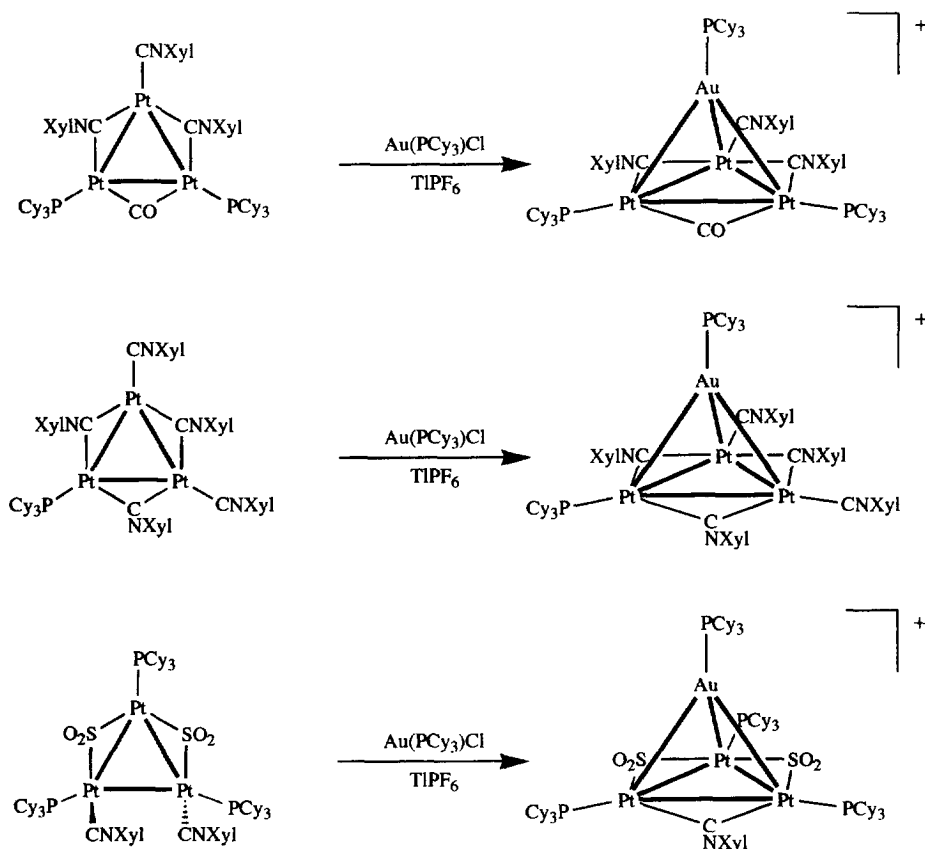Fig. 10. Molecular structure of the anion in $(AsPh_4)_2[Pt_3(\mu\text{-}CO)_3(CO)_3]_5$.

Scheme 10.

Scheme 11.

clusters. The Pt—Au bonding in the Pt_3Au_2 cluster can be described in terms of a 5-centre 2-electron bond. The interaction of the a_1 orbital of the Pt_3Au tetrahedron with the $Au(PR_3)$ fragment leads to reduced Pt—Pt and Pt—Au bonding character in the resulting molecular orbital, and consequently lower overlap population and longer bonds. Similar conclusions concerning the reduction in Pt—Au bonding on moving from Pt_3Au to Pt_3Au_2 can be made from the coupling constant data obtained from $^{31}P(^1H)$ NMR spectra. $^3J(P,P)$ between the phosphorus atoms on platinum and gold is reduced from 20 Hz to 0 Hz on coordination of the second AuP^+ fragment and $^2J(Pt,P)$ to the phosphorus atoms on gold is also reduced, from 250 to 190 Hz [76].

In the two examples where both the parent Pt_3 triangle and the Pt_3Au cluster have both been structurally characterized there is a small increase in the Pt—Pt bond distances from the parent Pt_3 triangles to the gold-capped triangles (Table 5). The increase in each bond length is a consequence of the decrease in overlap of the Pt binding orbitals owing to the presence of the electrophilic $AuPR_3$ fragment. The
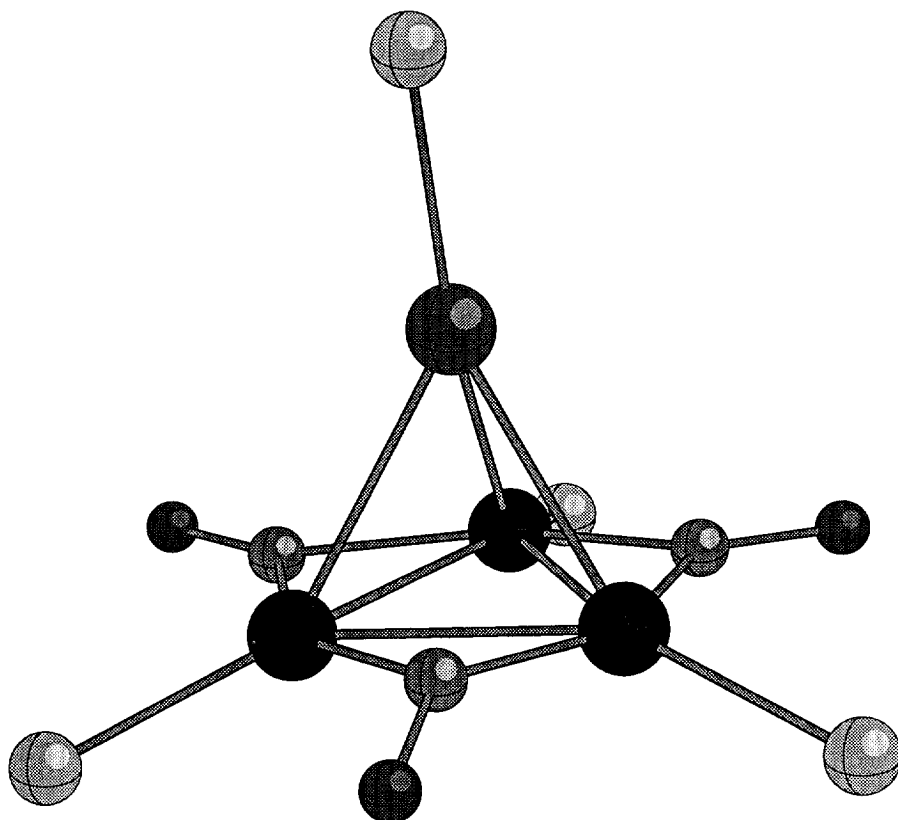
Fig. 11. Molecular structure of the cation in $[(Cy_3P)AuPt_3(\mu\text{-}CO)_3(PCy_3)_3]PF_6$, with cyclohexyl groups removed for clarity.

decrease in electronic charge density on the Pt atoms in the Pt_3Au cluster with respect to the Pt_3 cluster has been confirmed by X-ray photoelectron spectroscopy [80].

Dahmen and co-workers have noted that the stability of the gold-capped Pt_3 clusters decreases in the order $[Pt_3(\mu\text{-}CO)_3(PCy_3)_3] > [Pt_3(\mu\text{-}CO)(\mu\text{-}CNXyl)_2\text{-}(CNXyl)(PCy_3)_2] > [Pt_3(\mu\text{-}CNXyl)_3(CNXyl)_2(PCy_3)] > [Pt_3(\mu\text{-}CNXyl)_3(CNXyl)_3]$ [77]. This is of interest in the consideration of heterometallic cluster compounds as precursors for heterogeneous catalysts as the presence of phosphorus can lead to poisoning of the catalyst.

The 44-electron cluster $[Pt_3(\mu\text{-}SO_2)_2(CNXyl)_2(PCy_3)_3]$ cannot react with a gold phosphine fragment in the same manner as the clusters described above as the terminal isocyanide ligands partially block each face of the triangle. Reaction with $[Au(PCy_3)Cl]$ in the presence of $TlPF_6$ does occur and a combination of spectroscopic techniques suggests that an isocyanide ligand is lost during the course of the reaction, with the remaining isocyanide undergoing a change in coordination from terminal to bridging [78]. The IR spectrum shows $\nu(NC)$ at $1980\,\text{cm}^{-1}$ which is
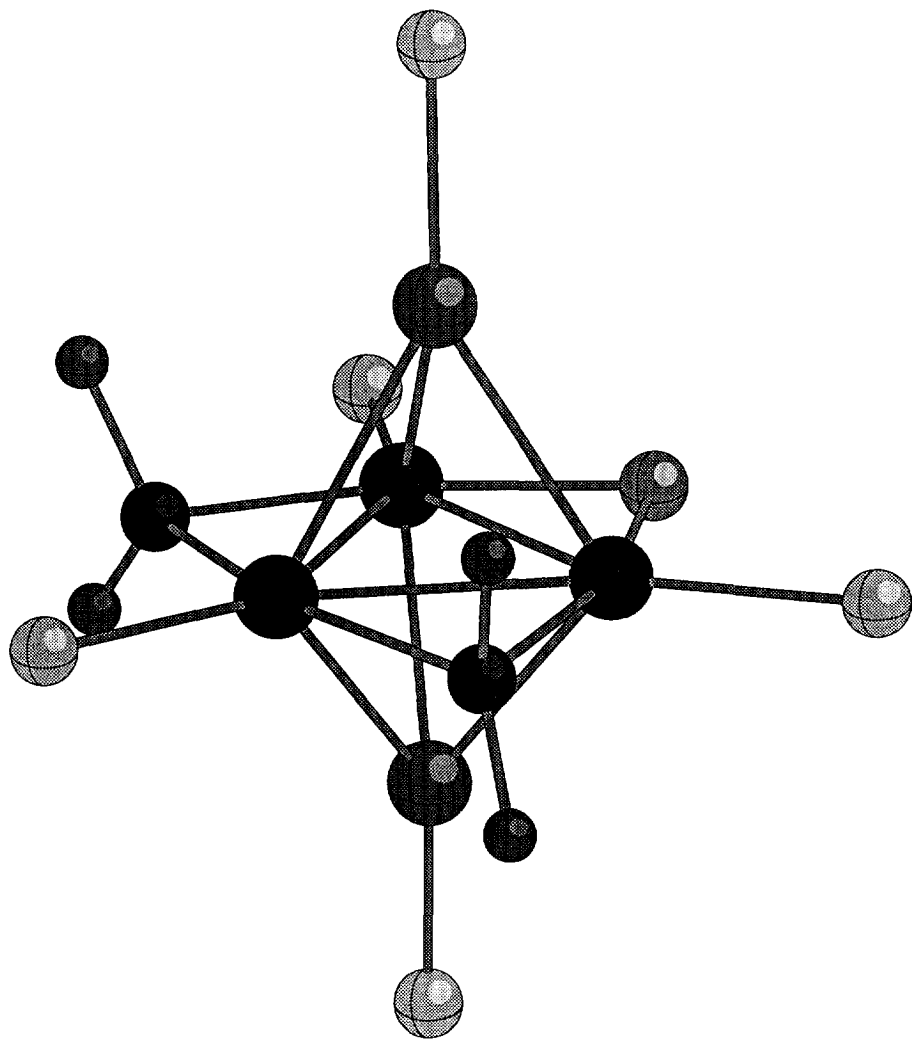
Fig. 12. Molecular structure of the cation in $[\{(C_6H_4F\text{-}p)_3PAu\}_2Pt_3(\mu\text{-}SO_2)_2(\mu\text{-}Cl)(PCy_3)_3]PF_6$, with p-fluorophenyl and cyclohexyl groups omitted for clarity.

consistent with a linear bridging isocyanide: this ligand has been observed in such a coordination mode and with a similar value for $\nu(NC)$ in the palladium clusters $[Pd_5(\mu\text{-}SO_2)_3(\mu\text{-}CNXyl)_2(CNXyl)_5]$ [81] and $[Pd_4(\mu\text{-}CNXyl)_4(\mu\text{-}OAc)_4]$ [82] but not before in a cluster of platinum. Unfortunately single crystals of diffraction quality have not been obtained and it has not been possible to confirm this formulation crystallographically.

The hydrido clusters of Puddephatt and co-workers also react with gold phosphine fragments [83]:
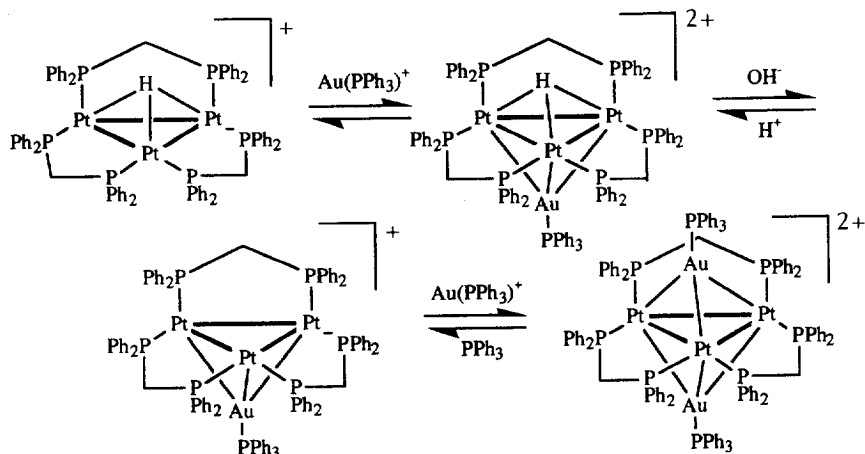
When both faces of the Pt_3 triangle are capped both electrophiles compete for the electron density of the a_1 bonding orbital of the Pt_3 triangle in much the same manner as in $[\{(C_6H_4F\text{-}p)_3PAu\}_2Pt_3(\mu\text{-}SO_2)_2(\mu\text{-}Cl)(PCy_3)_3]^+$. The ligands are more weakly bound than in complexes where only one side of the Pt_3 triangle is capped and this is illustrated by the reductions in $^1J(Pt,H)$ and $^2J(Pt,P(Au))]$ for the bis-capped clusters when compared with the mono-capped clusters [83].

14. Reactions with other metal electrophiles

The capping reactions described above are limited neither to the use of $AuPR_3$ fragments nor to 42-electron clusters. Other isolobal MPR_3 fragments such as $CuPR_3$

Table 4
Pt—Pt and Pt—Au bond distances for platinum–gold clusters

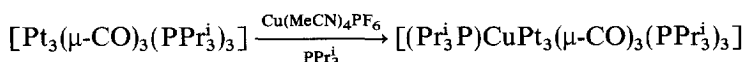|	Number of electrons	Pt—Pt (Å)	Pt—Au (Å)	Ref.
$[(Cy_3P)AuPt_3(\mu\text{-}CO)_3(PCy_3)_3]^+$	54	2.678(5), 2.704(6), 2.705(6)	2.750(5), 2.757(5), 2.768(5)	[74]
$[(Cy_3P)AuPt_3(\mu\text{-}CO)_2(\mu\text{-}SO_2)(PCy_3)_3]^+$	54	2.667(4), 2.680(4), 2.746(1)	2.755(1), 2.758(5), 2.759(5)	[75]
$[(Cy_3P)AuPt_3(\mu\text{-}CO)(\mu\text{-}CNXyl)_2(CNXyl)(PCy_3)_2]^+$	54	2.663(3), 2.663(3), 2.681(3)	2.777(3), 2.777(3), 2.781(4)	[77]
$[\{(C_6H_4F\text{-}p)_3P\}AuPt_3(\mu\text{-}SO_2)_2(\mu\text{-}Cl)(PCy_3)_3]$	56	2.851(1), 2.869(1), 2.872(1)	2.766(1), 2.769(1), 2.771(1)	[75]
$[\{(C_6H_4F\text{-}p)_3PAu\}_2Pt_3(\mu\text{-}SO_2)_2(\mu\text{-}Cl)(PCy_3)_3]^+$	68	2.884(2), 2.887(2), 2.888(2)	2.772(2), 2.776(2), 2.784(2), 2.775(2), 2.801(2), 2.803(2)	[76]

Table 5
Pt—Pt bond distances in Pt_3 and $AuPt_3$ clusters

	Pt—Pt (Å)	Pt—Pt in $Au(PCy_3)$ capped triangle (Å)	Ref.
$[Pt_3(\mu\text{-CO})_3(PCy_3)_3]$	2.653(2), 2.656(2), 2.656(2)	2.678(5), 2.704(6), 2.705(6)	[45,74]
$[Pt_3(\mu\text{-CO})(\mu\text{-CNXyl})_2(CNXyl)(PCy_3)_2]$	2.625(1), 2.627(1), 2.648(1)	2.663(3), 2.663(3), 2.681(3)	[50,77]

and $AgPR_3$ can be used in place of $AuPR_3$, for example [4]

$$[Pt_3(\mu\text{-CO})_3(PPr^i_3)_3] \xrightarrow[PPr^i_3]{Cu(MeCN)_4PF_6} [(Pr^i_3P)CuPt_3(\mu\text{-CO})_3(PPr^i_3)_3]$$

The 44-electron cluster compound $[Pt_3(\mu\text{-CO})_3(PCy_3)_2(dppp)]$ reacts with $AgCF_3SO_3$ to give a Pt_3Ag cluster [84] in which the silver atom caps the Pt_3 triangle and is weakly coordinated to one oxygen atom of the $CF_3SO_3^-$ anion:
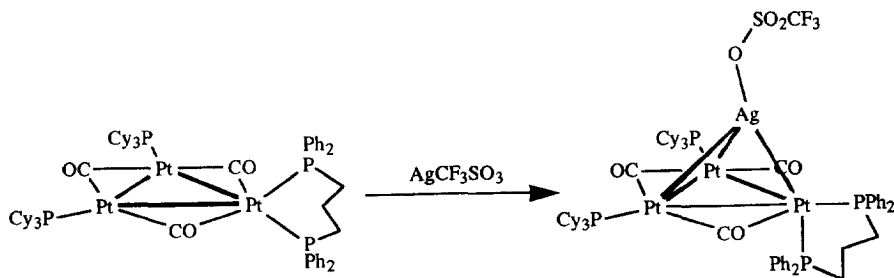
The tetrahedral core geometry of this cluster is distorted (Fig. 13), with one of the Pt—Pt bonds significantly shorter, at 2.653(2) Å, than the other two, which have lengths of 2.697(2) and 2.709(2) Å. Similarly, one Pt—Ag bond is, at 2.690(3) Å, considerably shorter than the other two, which have lengths of 2.919(4) and 2.927(3) Å. The shorter Pt—Ag bond is to the most sterically crowded platinum atom. This observation is consistent with the results of MO calculations. The replacement of a PtL fragment in $[Pt_3(\mu\text{-CO})_3L_3]$ by an angular PtL_2 fragment to form $[Pt_3(\mu\text{-CO})_3L_4]$ can be interpreted in terms of differences in the electronic characteristics of the fragments. Specifically, the PtL_2 fragment has a higher lying HOMO and a lower lying LUMO. The former contributes significantly to a high lying orbital in the $[Pt_3(\mu\text{-CO})_3L_4]$ cluster of b_1 symmetry. The higher localization of the Pt dp hybrid on the PtL_2 fragment and its hybrid character ensure that the overlap with the outpointing sp hybrid of the AgL fragment is larger for the sterically most crowded Pt and hence the shorter Pt—Ag bonds to this atom can be directly related to its higher nucleophilicity. These calculations also predict that the Pt—Pt bond
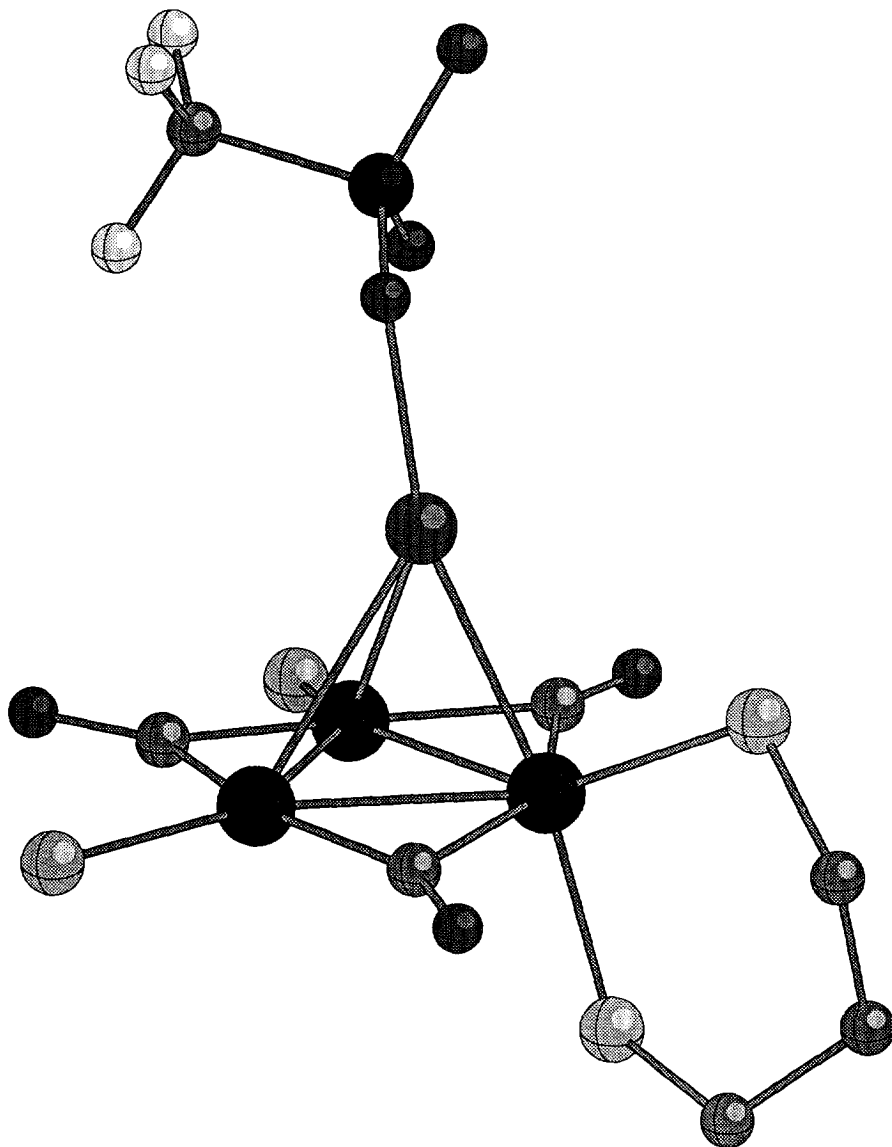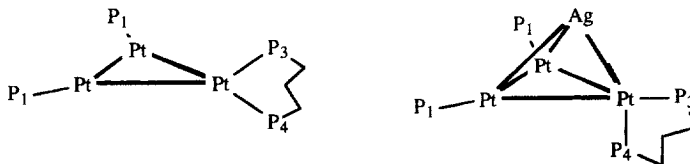
Fig. 13. Molecular structure of [(F$_3$CSO$_3$)AgPt$_3$(μ-CO)$_3$(PCy$_3$)$_2$(dppp)], with phenyl and cyclohexyl groups omitted for clarity.

opposite the PtL$_2$ fragment is shorter than the other Pt—Pt bonds, again borne out by the X-ray diffraction data [84].

Coordination of the Ag atom to one face of the triangle also leads to a distortion of the dppp ligand from its symmetrically chelating binding in [Pt$_3$(μ-CO)$_3$(PCy$_3$)$_2$(dppp)]. One Pt—P bond becomes closer to the plane of the Pt$_3$ triangle away from the silver atom whereas the other becomes nearer the
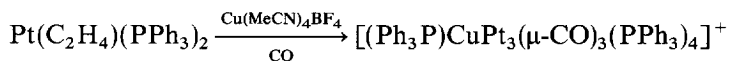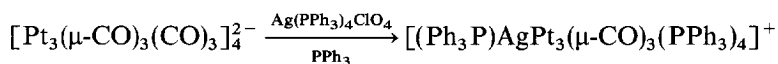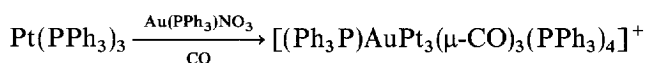
Table 6

Nuclear magnetic resonance coupling constants for $[Pt_3(\mu\text{-}CO)_3(PCy_3)_2(dppp)]$ and $[(F_3CSO_3)AgPt_3(\mu\text{-}CO)_3(PCy_3)_2(dppp)]$

$^3J(P_1-P_3)$ (Hz)	19	51
$^3J(P_1-P_4)$ (Hz)	19	6
$^2J(Pt_1-P_3)$ (Hz)	270	393
$^2J(Pt_1-P_4)$ (Hz)	270	88
$^2J(Ag-P_3)$ (Hz)		30
$^2J(Ag-P_4)$ (Hz)		192

perpendicular. Such distortions are apparent from a comparison of the coupling constants observed in the $^{31}P(^1H)$ NMR spectrum for the Pt_3Ag cluster with those of the parent *triangulo*-Pt_3 cluster shown in Table 6. Coupling constants for P_3 with P_1 and P_2, and with Pt_1 and Pt_2, become larger in the Pt_3Ag cluster whereas those for P_4 with the same atoms are decreased. The $Ag-Pt_3-P_4$ bond angle is 170.2(3)° leading to a high $^2J(Ag-P)$ coupling constant whereas the $Ag-Pt_3-P_3$ bond angle is 91.3° which results in a considerably lower coupling constant.

Related 56-electron cluster compounds of the general formula $[(Ph_3P)MPt_3(\mu\text{-}CO)_3(PPh_3)_4]^+$ have been prepared for M = Au [85], Ag [86] and Cu [87], either from the reactions of monomeric fragments or from $[Pt_3(\mu\text{-}CO)_3(CO)_3]_4^{2-}$

$$Pt(PPh_3)_3 \xrightarrow[CO]{Au(PPh_3)NO_3} [(Ph_3P)AuPt_3(\mu\text{-}CO)_3(PPh_3)_4]^+$$

$$[Pt_3(\mu\text{-}CO)_3(CO)_3]_4^{2-} \xrightarrow[PPh_3]{Ag(PPh_3)_4ClO_4} [(Ph_3P)AgPt_3(\mu\text{-}CO)_3(PPh_3)_4]^+$$

$$Pt(C_2H_4)(PPh_3)_2 \xrightarrow[CO]{Cu(MeCN)_4BF_4} [(Ph_3P)CuPt_3(\mu\text{-}CO)_3(PPh_3)_4]^+$$

Crystal structures of these clusters show similar distortions in the metal framework, with the $Pt-M$ bond to the most sterically crowded platinum atom considerably shorter than those to the other two platinum atoms.

15. Reactions with thallium(1+) and mercury

$[Pt_3(\mu\text{-}CO)_3(PCy_3)_3]$ reacts with $TlPF_6$ to form a thallium-capped triangle [88]:
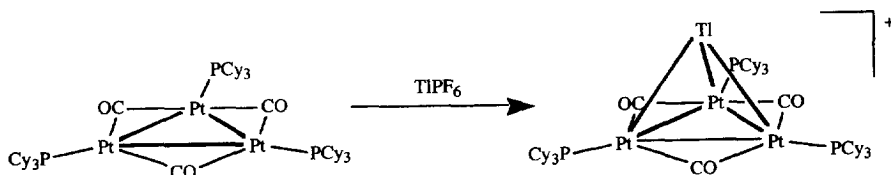
Initial reactions were undertaken in the presence of $[Rh(COD)Cl]_2$ and crystals obtained from this reaction mixture showed the thallium atom weakly coordinated (Tl—Cl distance, 2.981(9) Å) to the two chlorine atoms of an $[Rh(COD)Cl_2]$ anion. The Pt—Pt bond distances are slightly greater (2.667(1) 2.668(1) Å) than in the parent *triangulo* cluster. The Pt—Tl bond distances are 3.034(1) and 3.047(1) Å, considerably longer than the Pt—Au distances in related 54-electron Pt_3Au clusters, clearly reflecting the effect of the filled 6s shell. The $^{31}P(^1H)$ NMR spectrum showed the presence of a $^2J(Pt,Tl)$ coupling constant of 193 Hz at room temperature, demonstrating the retention of the capping thallium atom in solution. However, the thallium is sufficiently labile to be replaced by other capping metal atoms [88], for example

$$[TlPt_3(\mu\text{-}CO)_3(PCy_3)_3]^+ \xrightarrow{\ Au(PCy_3)Cl\ } [(Cy_3P)AuPt_3(\mu\text{-}CO)_3(PCy_3)_3]^+$$
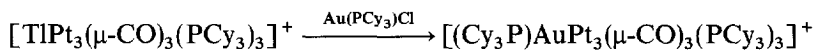
$[Pt_3(\mu\text{-}CO)_3(PR_3)_3]$ ($PR_3 = PPhPr_2^i$, PPr_3^i, PEt_2Bu^t) react with metallic mercury [89] giving blue–green solutions from which dark violet crystals could be obtained:
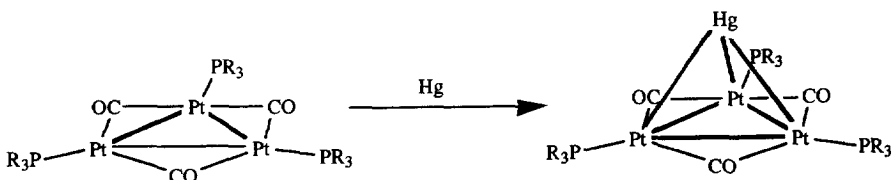

The crystal structure of the $PPhPr_2^i$ derivative consists of two triangular $[Pt_3(\mu\text{-}CO)_3(PR_3)_3]$ units, each capped by a mercury atom, with the two units joined through the mercury atoms [89] (Fig. 14), which are at a distance of 3.225(1) Å, considerably longer than the Hg—Hg separation either in the α crystalline form of Hg (2.99 Å) or in Hg_2X_2 salts (2.49–2.51 Å for X = halide [90]). Pt—Pt bond distances within the Pt_3 triangles are slightly longer than those found in $[Pt_3(\mu\text{-}CO)_3(PCy_3)_3]$ and the Pt—Hg distances are, at 2.931(1)–3.084(1) Å, comparable with the Pt—Tl distances discussed above.

^{31}P, ^{195}Pt and ^{199}Hg NMR studies show that the mixed-metal clusters are fluxional even at −90 °C and the cluster is believed to be monomeric in solution [91]. The bonding between the Hg_2 unit and the Pt_3 fragment can be described as a linear combination of the two empty a_1 orbitals on the Pt_3 fragments and the two filled 6s orbitals on the Hg atoms. This gives one strongly bonding and one weakly

bonding MO, accommodating the four bonding electrons. It is likely that the residual charge on the thallium prevents a similar dimerization for $[TlPt_3(\mu\text{-}CO)_3(PCy_3)_3]^+$.

The cluster compound $[Pt_3(\mu_3\text{-}CO)(\mu\text{-}dppm)_3]^{2+}$ also reacts with metallic mercury [92]:
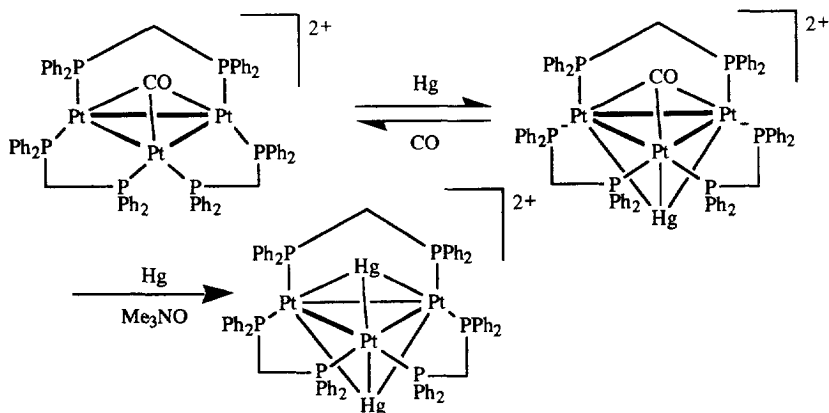
Addition of Me_3NO in the presence of excess mercury to $[HgPt_3(\mu_3\text{-}CO)\text{-}(\mu\text{-}dppm)_3]^{2+}$ gives the bis-mercury capped cluster $[Hg_2Pt_3(\mu\text{-}dppm)_3]^{2+}$. The Pt—Hg bonds in these compounds are labile and the mercury atoms are readily displaced, for example by reaction with CO which regenerates $[Pt_3(\mu_3\text{-}CO)(\mu\text{-}dppm)_3]^{2+}$ presumably via the bis-carbonyl adduct. The crystal structure of $[HgPt_3(\mu_3\text{-}CO)(\mu\text{-}dppm)_3](PF_6)_2$ has Pt—Hg bond distances of between 2.860(1) and 2.974(1) Å [92].

16. Reactions with metal halides

The ability of *triangulo* platinum cluster compounds to form "addition compounds" can be extended to reactions with metal halides of groups 11, 12 and 13 [93]:

MX_n = CuCl, CuBr, CuI, $ZnBr_2$, ZnI_2, $CdBr_2$, CdI_2, $InBr_3$

PR_3 = PPr^i_3, $PPhPr^i_2$
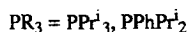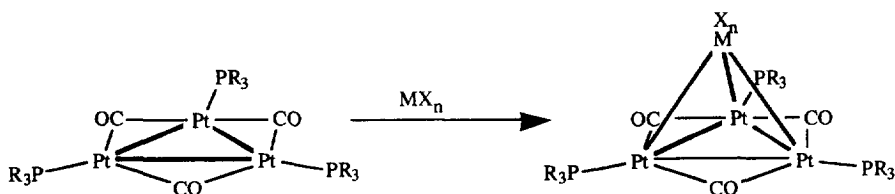
Fig. 14. Molecular structure of [HgPt$_3$(μ-CO)$_3$(PPhPr$_2^i$)$_3$]$_2$, with phenyl and iso-propyl groups omitted for clarity.

The X-ray crystal structure for the cluster [I$_2$ZnPt$_3$(μ-CO)$_3$(PPhPr$_2^i$)$_3$] shows the ZnI$_2$ moiety unsymmetrically placed above the Pt$_3$ triangle with the iodine atoms defining angles of 66.1° and 48.1° with the axis linking the centre of the Pt$_3$ triangle and the Zn atom (Fig. 15). The plane defined by ZnI$_2$ goes through one platinum atom and bisects the bond linking the other two. There are two short Pt—Zn distances of 2.624(5) and 2.650(5) Å and one longer distance of 2.755(5) Å, but only slight differences are observed in the Pt—Pt distances. While two of the phosphorus atoms are slightly below the Pt$_3$ plane (10°), the third shows a greater distortion (38°) because of steric interactions with one of the iodine atoms.

Mercury(I) and mercury(II) halides also react with *triangulo*-platinum clusters [91]:
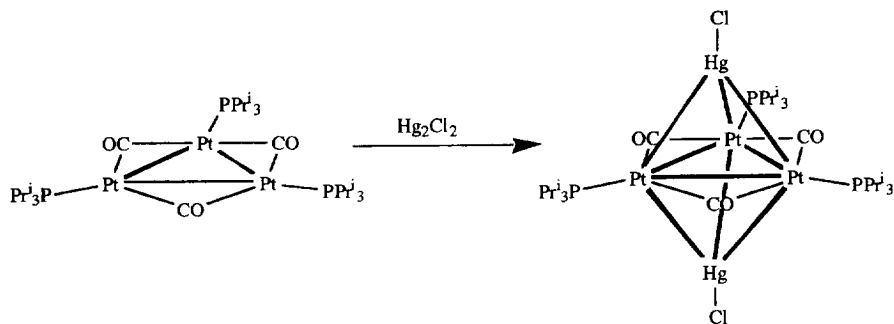
The main cluster products are identical in both cases but for HgX_2 the reaction involves a redox process and there are also Pt(I) and Pt(II) byproducts formed. ^{31}P and ^{195}Pt NMR studies show that the product, $[(XHg)_2Pt_3(\mu\text{-CO})_3(PR_3)_3]$, is monomeric in solution. However, an X-ray crystallographical analysis of $[(BrHg)_2Pt_3(\mu\text{-CO})_3(PPhCy_2)_3]$ has revealed that the compound occurs as a halide bridged dimer, $[\{(BrHg)Pt_3(\mu\text{-CO})_3(PPhCy_2)_3\}_2\{\mu\text{-HgBr}\}_2]$ in the solid state, as
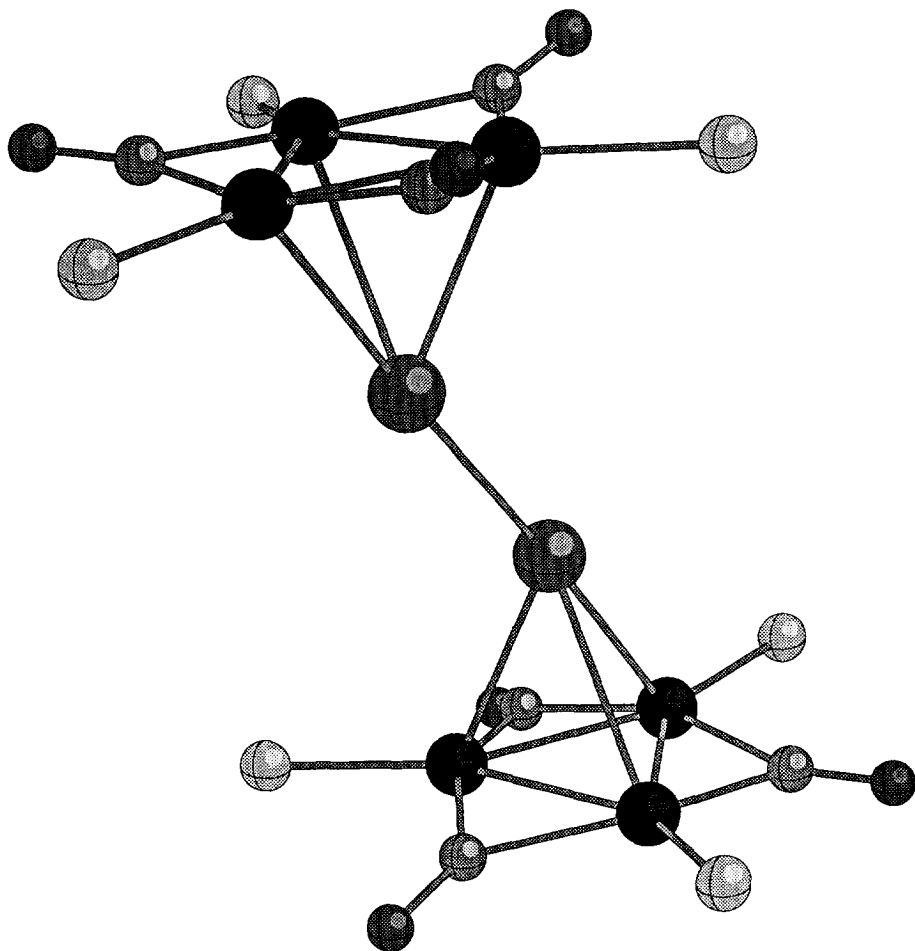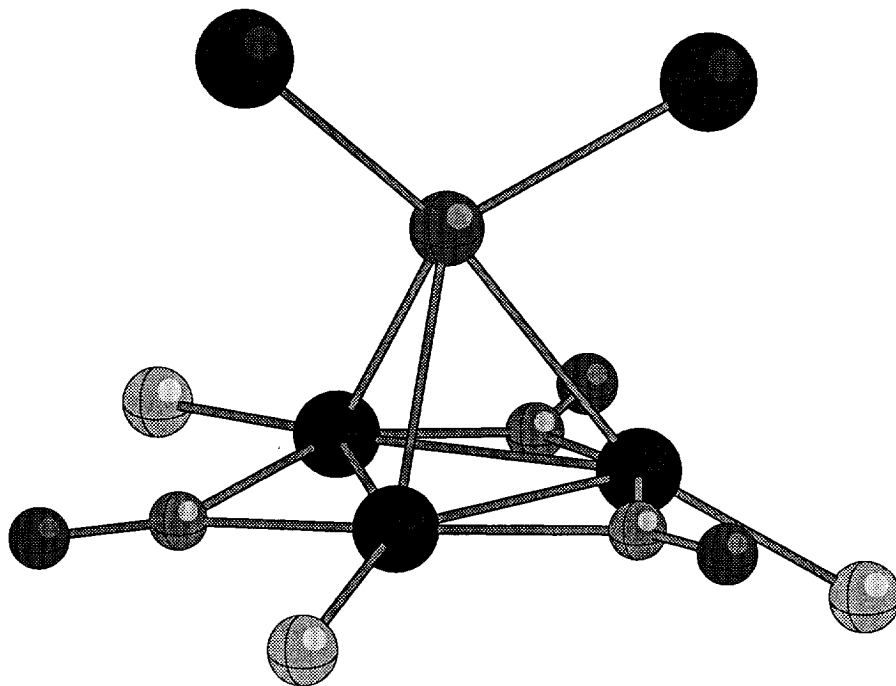

Fig. 15. Molecular structure of $[I_2ZnPt_3(\mu\text{-CO})_3(PPhPr_2^i)_3]$, with phenyl and iso-propyl groups omitted for clarity.

shown in Fig. 16. Hence the central part of the cluster core consists of a square-planar arrangement of two mercury atoms and two bridging bromine atoms, with each mercury atom additionally bonded to a *triangulo*-platinum unit which is capped on the other face by a HgBr fragment. The Pt—Pt bond distances within this compound, 2.656(1) Å, are comparable with those observed for other heterometallic clusters containing the $Pt_3(\mu\text{-CO})_3(PR_3)_3$ unit. Pt—Hg distances to the central mercury atoms, bonded to the bridging bromides, are slightly longer (2.853(1) Å) than those to the capping mercury atoms (2.834(1) Å).

The Pt—Pt distances are considerably shorter than in $[\{(C_6H_4F\text{-}p)_3PAu\}_2Pt_3\text{-}(\mu\text{-SO}_2)_2(\mu\text{-Cl})(PCy_3)_3]^+$ [76] although both cluster compounds formally are associated with 68 bonding electrons. This is because the HOMO in $[(XHg)_2Pt_3(\mu\text{-CO})_3(PR_3)_3]$ is an a_2'' MO which is weakly Pt—Pt and Pt—Hg bonding [91], whereas the HOMO for $[(R_3PAu)_2Pt_3(\mu\text{-SO}_2)_2(\mu\text{-Cl})\text{-}(PR_3)_3]^+$ is an a_2' MO which is Pt—Pt antibonding. This orbital is stabilized for $[(R_3PAu)_2Pt_3(\mu\text{-SO}_2)_2(\mu\text{-Cl})(PR_3)_3]^+$ by the bridging SO_2 and Cl ligands. Calculations on $[(XHg)_2Pt_3(\mu\text{-CO})_3(PR_3)_3]$ show little difference in the frontier orbitals between the monomer and dimer and suggest little change in the metal–metal bonding on dimerization.

17. Sandwich clusters

If instead of reacting with an ML or MX_n fragment, a *triangulo*-platinum cluster is reacted in the appropriate stoichiometry with an "M^+" fragment, then a sandwich cluster complex with two Pt_3 fragments joined by the M^+ ion can result [94,95] (Scheme 12). Problems with competing phosphine abstraction reactions were observed using $[Pt_3(\mu\text{-CO})_3(PCy_3)_3]$. These were avoided by using $[Pt_3(\mu\text{-CO})_3(PPh_3)_4]$ which contains an additional phosphine ligand [95].

There are some differences in the structures of the Ag, Cu and Au clusters. The two Pt_3 triangles for the copper and gold (Fig. 17) compounds are twisted from an eclipsed D_{3h} conformation by similar angles (21.5° and 22.3°) [95] whereas for the silver compound they adopt a staggered conformation (60°) [94]. Theoretical studies have indicated that clusters with layers of platinum triangles and interstitial atoms possess very low rotational barriers [71], and solid state structures could be dominated by the phosphine ligands or influenced by crystal packing effects.

In $[Ag\{Pt_3(\mu\text{-CO})_3(PPr_3^i)_3\}_2]^+$ one Pt—Pt bond distance is slightly shorter than the other two although for $[Cu\{Pt_3(\mu\text{-CO})_3(PPh_3)_3\}_2]^+$ and $[Au\{Pt_3(\mu\text{-CO})_3(PPh_3)_3\}_2]^+$ all the Pt—Pt distances are equivalent. In all cases they lie within the normal range for 42-electron *triangulo* clusters. The mean Pt—Au distance in $[Au\{Pt_3(\mu\text{-CO})_3(PPh_3)_3\}_2]^+$ is slightly shorter, 2.728 Å, than that found in the tetrahedral Pt_3Au clusters. In all cases the carbonyl ligands are distorted towards the central atom and the phosphorus atoms away from the central atom.

The primary bonding interactions result from the overlap of the Pt_3 ring orbitals and the s valence orbital of the group 11 atom. A 3-centre orbital interaction results and, in $[M\{Pt_3(\mu\text{-CO})_3(PR_3)_3\}_2]^+$ which contains 94 bonding electrons, only the most stable in-phase combination is occupied. The related compound
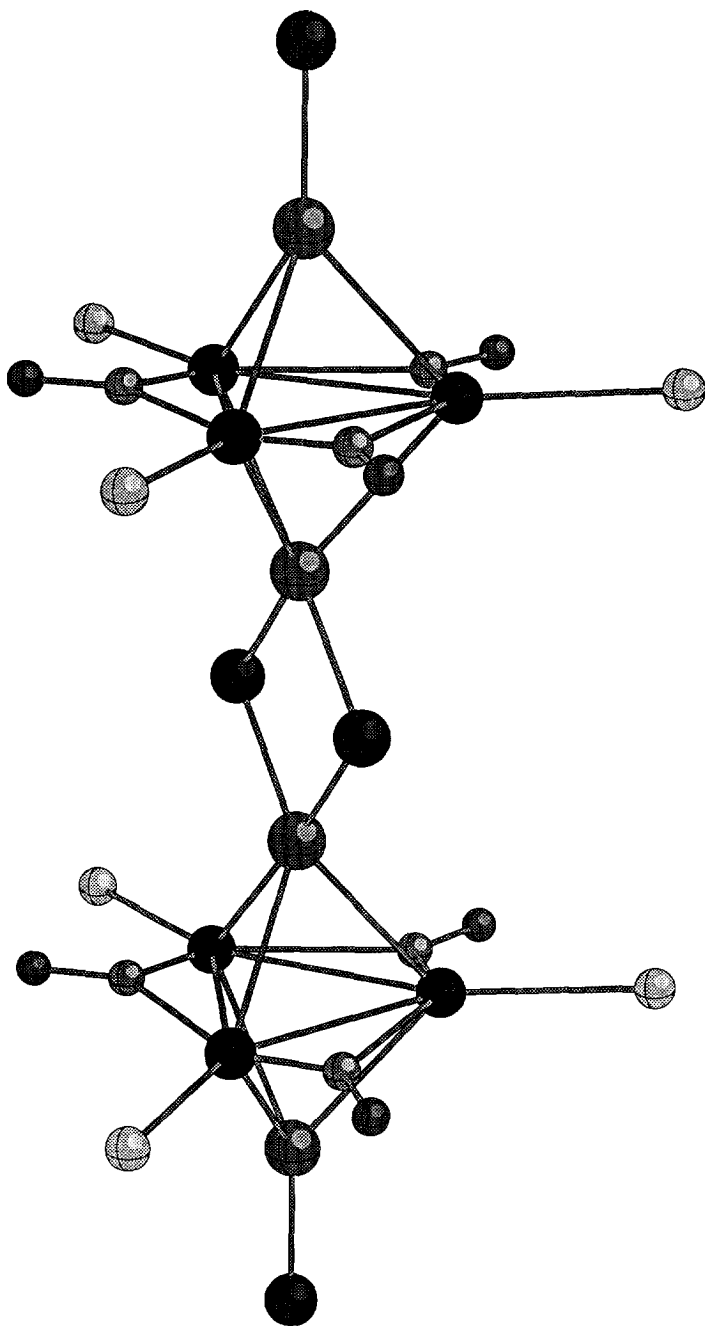
Fig. 16. Molecular structure of [{(BrHg)Pt$_3$(μ-CO)$_3$(PPhCy$_2$)$_3$}$_2${μ-HgBr}$_2$], with phenyl and cyclohexyl groups omitted for clarity.
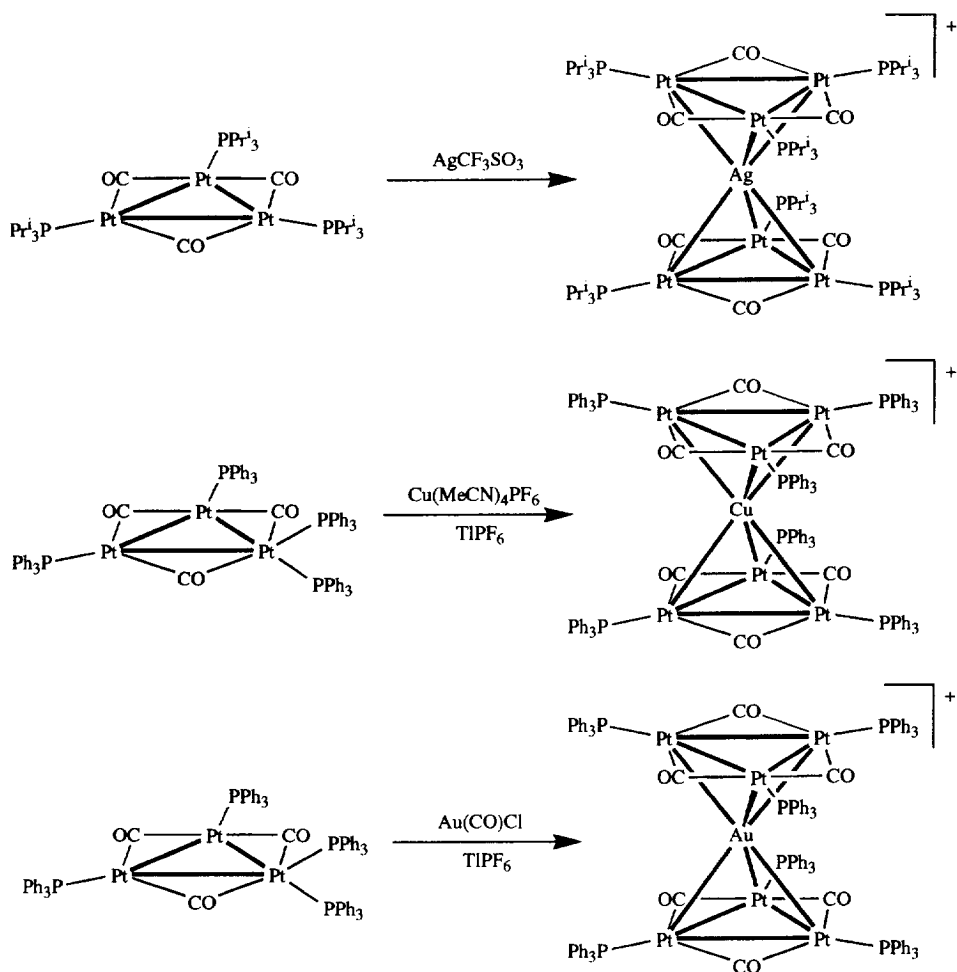
Scheme 12.

[Hg{Pt$_3$(μ-CNXyl)$_3$(CNXyl)$_3$}$_2$]   [96a],   synthesized   from   the   sodium amalgam reduction of PtCl$_2$(XylNC)$_2$, contains 96 valence electrons. In this case an additional orbital of a$_2''$ symmetry located primarily on the Pt$_3$ triangles is occupied.   [Hg{Pt$_3$(μ-CNXyl)$_3$(CNXyl)$_3$}$_2$]   has   also   been   obtained   from [Pt$_3$(μ-CNXyl)$_3$(CNXyl)$_3$] and sodium amalgam in the presence of XylNC [96b].

Related Hg and Hg$_2$ sandwich clusters supported by long chain diphosphine ligands have been prepared from the sodium amalgam reduction of [Pt(COD)Cl$_2$] in the presence of XylNC and a diphosphine [97]. The reaction products depend on the length of the diphosphine chain. When the methylene chain is long enough ($n = 5$ or 6) it links the two Pt$_3$ triangles incorporating Hg$_2$ whereas for an intermediate length ($n = 4$) only one mercury atom is incorporated (Scheme 13). For shorter diphosphines ($n = 2, 3$) no mixed-metal clusters are obtained.
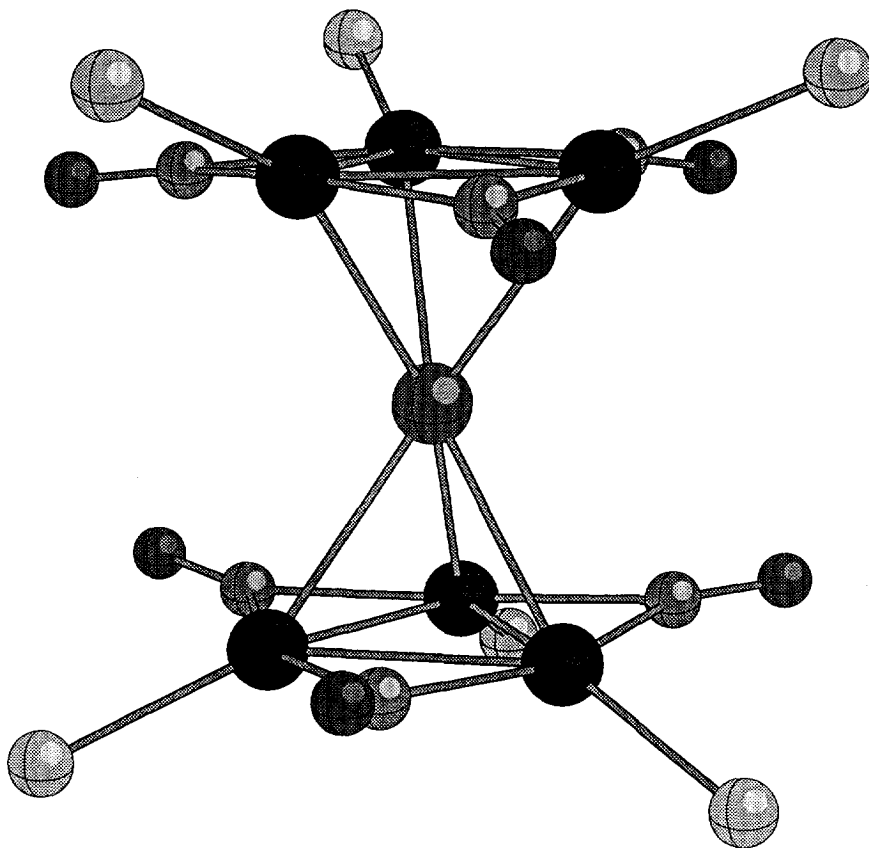
Fig. 17. Molecular structure of the cation of $[Au\{Pt_3(\mu\text{-}CO)_3(PPh_3)_3\}_2]PF_6$, with phenyl groups omitted for clarity.

The crystal structure of $[Hg_2\{Pt_3(\mu\text{-}CNXyl)_3\}_2(dpphex)_3]$ shows slightly shorter Hg—Pt distances than in $[Hg\{Pt_3(\mu\text{-}CNXyl)_3(CNXyl)_3\}_2]$, perhaps because of the chelating effect of the diphosphine ligands. The Hg—Hg bond distance is, at 2.872(7) Å, considerably shorter than in the structure of $[Hg_2\{Pt_3(\mu\text{-}CO)_3(PPhPr^i_2)_3\}_2]$ discussed above. No sandwich compound of the general formula $[Hg\{Pt_3(\mu\text{-}CO)_3(PR_3)_3\}_2]$ has yet been reported. However, the palladium analogue $[Hg\{Pd_3(\mu\text{-}CO)_3(PEt_3)_3\}_2]$ has been synthesized, but only characterized spectroscopically [98].

18. Conclusions

Since Chatt and Chini's initial important contribution platinum *triangulo* cluster chemistry has developed significantly and shown a diversity in reactivity which is almost unique. Specifically, the following features are noteworthy.
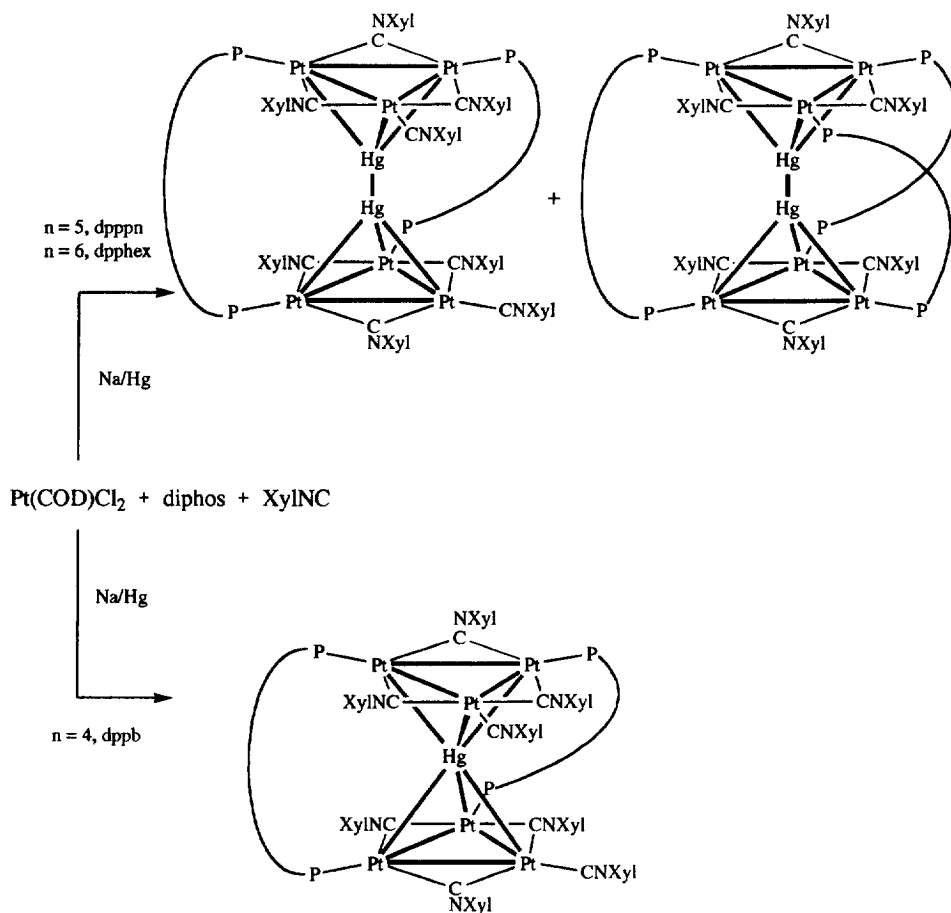
Scheme 13.

(1) The platinum *triangulo* cluster compounds may be formed with a range of phosphines, isocyanides, carbonyls as terminal ligands and carbonyls, nitrosyls, isocyanides, sulphur dioxide, phosphides, halides, thiolates as bridging ligands. This means that the electronic and steric environment of the platinum cluster may be modified and tuned over a wide range.

(2) The disposition of terminal and bridging ligands in the metal triangular plane leaves the two faces of the triangle available for the addition of interesting substrates.

(3) The *triangulo*-metal clusters $[Pt_3(\mu\text{-}X)_3(PR_3)_3]$ and $[Pt_3(\mu\text{-}CO)_3(CO)_3]$ have empty metal orbitals in the frontier orbital region which enable them to accommodate additional electrons. Therefore, both 42- and 44-electron *triangulo* clusters may be formed. There are two closely spaced available orbitals which lie perpendicular or within the plane and which have different bonding characteristics with respect to the metal triangle. The electrons which are donated to these orbitals may be either

donated by lone pairs from terminal or bridging ligands, or contributed by an increase in the negative charge on the cluster.

(4) The availability of these orbitals makes the substitution chemistry of 42-electron *triangulo* clusters facile, because the activation energy for the formation of the intermediate 44-electron cluster is small. Therefore, there are examples of phosphine exchange and bridging ligand exchange which occur at room temperature. More interestingly, the phosphine ligands may be replaced by sterically demanding ligands such as isocyanides.

(5) The availability of filled or empty orbitals in the frontier region makes the platinum triangles amphoteric. Specifically, the metal triangle reacts with metal electrophiles, e.g. $AuPR_3^+$, and main group and metallic nucleophiles, e.g. R_3P, Hg and halide anions.

(6) The empty orbital of a_2'' symmetry in $[Pt_3(\mu\text{-}CO)_3(CO)_3]$ which lies perpendicular to the metal plane may be utilised in the formation of stacked platinum *triangulo* clusters, $[Pt_3(\mu\text{-}CO)_3(CO)_3]_n^{2-}$.

References

[1] D.F. Schriver, H.D. Kaesz and R.D. Adams, The Chemistry of Metal Cluster Complexes, VCH, New York, 1990.

[2] D.M.P. Mingos and D.J. Wales, Introduction to Cluster Chemistry, Prentice-Hall, Englewood Cliffs, NJ, 1990.

[3] D.M.P. Mingos and R.W.M. Wardle, Transition Met. Chem., 10 (1985) 441.

[4] D. Imhof and L.M. Venanzi, Chem. Soc. Rev., 23 (1994) 185.

[5] G. Booth and J. Chatt, J. Chem. Soc. A, (1966) 634.

[6] J. Chatt and P. Chini, J. Chem. Soc. A, (1970) 1538.

[7] H.C. Clark, A.B. Goel and C.S. Wong, Inorg. Chim. Acta, 34 (1979) 159.

[8] R.G. Goel, W.O. Ogini and R.C. Srivastava, Organometallics, 1 (1982) 819.

[9] D.G. Evans, M.F. Hallam, D.M.P. Mingos and R.W.M. Wardle, J. Chem. Soc., Dalton Trans., (1987) 1889.

[10] K.-H. Dahmen, A. Moor, R. Naegeli and L.M. Venanzi, Inorg. Chem., 30 (1991) 4285.

[11] A. Moor, P.S. Pregosin and L.M. Venanzi, Inorg. Chim. Acta, 48 (1981) 153.

[12] A. Moor, P.S. Pregosin and L.M. Venanzi, Inorg. Chim. Acta, 61 (1982) 135.

[13] T. Yoshida and S. Otsuka, J. Am. Chem. Soc., 99 (1977) 2134.

[14] P.W. Frost, J.A.K. Howard, J.L. Spencer, D.G. Turner and D. Gregson, J. Chem. Soc., Chem. Commun., (1981) 1104.

[15] D. Gregson, J.A.K. Howard, M. Murray and J.L. Spencer, J. Chem. Soc., Chem. Commun., (1981) 716.

[16] J.M. Ritchey and D.C. Moody, Inorg. Chim. Acta, 74 (1983) 271.

[17] J.L. Haggitt and D.M.P. Mingos, J. Organomet Chem., 462 (1993) 365.

[18] M. Green, J.A.K. Howard, M. Murray, J.L. Spencer and F.G.A. Stone, J. Chem. Soc., Dalton Trans., (1977) 1509.

[19] G. Ferguson, B.R. Lloyd and R.J. Puddephatt, Organometallics, 5 (1986) 344.

[20] A.D. Burrows and D.M.P. Mingos, Transition Met. Chem., 18 (1993) 129.

[21] B.R. Lloyd and R.J. Puddephatt, Inorg. Chim. Acta, 90 (1984) L77.

[22] M. Hidai, M. Kokura and Y. Uchida, J. Organomet. Chem., 52 (1973) 431.

[23] K. Kudo, M. Hidai and Y. Uchida, J. Organomet. Chem., 33 (1971) 393.

[24] A. Christofides, J. Organomet. Chem., 259 (1983) 355.

[25] S. Otsuka, Y. Tatsuno, M. Miki, T. Aoki, M. Matsumoto, H. Yoshioka and K. Nakatsu, J. Chem. Soc., Chem. Commun., (1973) 445.

[26] G.W. Bushnell, K.R. Dixon, P.M. Moroney, A.D. Rattray and C. Wan, J. Chem. Soc., Chem. Commun., (1977) 709.

[27] D.M.P. Mingos, Acc. Chem. Res., 17 (1984) 311.

[28] F.R. Hartley, in G. Wilkinson, F.G.A. Stone and E.W. Abel (eds.), Comprehensive Organometallic Chemistry, Vol. 6, Pergamon, Oxford, 1982, p. 471.

[29] D.G. Evans and D.M.P. Mingos, J. Organomet. Chem., 240 (1982) 321.

[30] D.G. Evans, J. Organomet. Chem., 319 (1987) 265.

[31] C. Mealli, J. Am. Chem. Soc., 107 (1985) 2245.

[32] D.G. Evans, J. Organomet. Chem., 352 (1988) 397.

[33] D.G. Evans, J. Chem. Soc., Chem. Commun., (1983) 675.

[34] D.M.P. Mingos and T. Slee, J. Organomet. Chem., 394 (1990) 679.

[35] C.E. Briant, D.G. Evans and D.M.P. Mingos, J. Chem. Soc., Dalton Trans., (1986) 1535.

[36] M. Green, R.M. Mills, G.N. Pain, F.G.A. Stone and P. Woodward, J. Chem. Soc., Dalton Trans., (1982) 1309.

[37] R. Bender and P. Braunstein, J. Chem. Soc., Chem. Commun., (1983) 334.

[38] S.G. Bott, M.F. Hallam, O.J. Ezomo, D.M.P. Mingos and I.D. Williams, J. Chem. Soc., Dalton Trans., (1988) 1461.

[39] S.G. Bott, A.D. Burrows, O.J. Ezomo, M.F. Hallam, J.G. Jeffrey and D.M.P. Mingos, J. Chem. Soc., Dalton Trans., (1990) 3335.

[40] C.S. Browning, D.H. Farrar, R.R. Gukathasan and S.A. Morris, Organometallics, 4 (1985) 1750.

[41] R.A. Burrow, D.H. Farrar and J.J. Irwin, Inorg. Chim. Acta, 181 (1991) 65.

[42] C.A. Tolman, Chem. Rev., 77 (1977) 313.

[43] A. Albinati, G. Carturan and A. Musco, Inorg. Chim. Acta, 16 (1976) L3.

[44] M.F. Hallam, N.D. Howells, D.M.P. Mingos and R.W.M. Wardle, J. Chem. Soc., Dalton Trans., (1985) 845.

[45] A. Albinati, Inorg. Chim. Acta, 22 (1977) L31.

[46] J. Anbei and C. Qiuzi, Jiegou Huaxue (J. Struct. Chem.), 4 (1985) 96.

[47] J.C. Calabrese, L.F. Dahl, P. Chini, G. Longoni and S. Martinengo, J. Am. Chem. Soc., 96 (1974) 2614.

[48] D.C. Moody and R.R. Ryan, Inorg. Chem., 16 (1977) 1052.

[49] N.M. Boag, J. Browning, C. Crocker, P.L. Goggin, R.J. Goodfellow, M. Murray and J.L. Spencer, J. Chem. Res. (S), (1978) 228; J. Chem. Res. (M), (1978) 2962.

[50] C.E. Briant, D.I. Gilmour, D.M.P. Mingos and R.W.M. Wardle, J. Chem. Soc., Dalton Trans., (1985) 1693.

[51] D.M.P. Mingos, I.D. Williams and M.J. Watson, J. Chem. Soc., Dalton Trans., (1988) 1509.

[52] J.L. Haggitt and D.M.P. Mingos, J. Chem. Soc., Dalton Trans., (1994) 1013.

[53] J.M. Forward, D.Phil. Thesis, University of Oxford, 1993.

[54] S.J. Cartwright, K.R. Dixon and A.D. Rattray, Inorg. Chem., 19 (1980) 1120.

[55] D.J. Sherman, D.Phil. Thesis, University of Oxford, 1987.

[56] A.D. Burrows, J.C. Machell and D.M.P. Mingos, J. Chem. Soc., Dalton Trans., (1992) 1939.

[57] P. Braunstein and A.D. Burrows, unpublished results, 1993.

[58] K.R. Dixon and A.D. Rattray, Inorg. Chem., 17 (1978) 1099.

[59] N. Hadj-Bagheri, J. Browning, K. Dehghan, K.R. Dixon, N.J. Meanwell and R. Vefghi, J. Organomet. Chem., 396 (1990) C47.

[60] R.J. Puddephatt, Lj. Manojlovic-Muir and K.W. Muir, Polyhedron, 9 (1990) 2767.

[61] M.C. Jennings, R.J. Puddephatt, Lj. Manojlovic-Muir, K.W. Muir and B.N. Mwariri, Organometallics, 11 (1992) 4164.

[62] B.R. Lloyd, Lj. Manojlovic-Muir, K.W. Muir and R.J. Puddephatt, Organometallics, 12 (1993) 1231.

[63] M. Rashidi, E. Kristof, J.J. Vittal and R.J. Puddephatt, Inorg. Chem., 33 (1994) 1497.

[64] A.M. Bradford, N.C. Payne, R.J. Puddephatt, D.-S. Yang and T.B. Marder, J. Chem. Soc., Chem. Commun., (1990) 1462.

[65] A.M. Bradford, G. Douglas, Lj. Manojlovic-Muir, K.W. Muir and R.J. Puddephatt, Organometallics, 9 (1990) 409.

[66] S.S.M. Ling, N. Hadj-Bagheri, Lj. Manojlovic-Muir, K.W. Muir and R.J. Puddephatt, Inorg. Chem., 26 (1987) 231. A.M. Bradford and R.J. Puddephatt, New J. Chem., 12 (1988) 427.

[67] G. Douglas, M.C. Jennings, Lj. Manojlovic-Muir, K.W. Muir and R.J. Puddephatt, J. Chem. Soc., Chem. Commun., (1989) 159.

[68] G. Ferguson, B.R. Lloyd, Lj. Manojlovic-Muir, K.W. Muir and R.J. Puddephatt, Inorg. Chem., 25 (1986) 4190.

[69] A.M. Bradford, R.J. Puddephatt, G. Douglas, Lj. Manojlovic-Muir and K.W. Muir, Organometallics, 9 (1990) 1579.

[70] G. Longoni and P. Chini, J. Am. Chem. Soc., 98 (1976) 7225.

[71] D.J. Underwood, R. Hoffmann, K. Tatsumi, A. Nakamura and Y. Yamamoto, J. Am. Chem. Soc., 107 (1985) 5968.

[72] C. Brown, B.T. Heaton, A.D.C. Towl, P. Chini, A. Fumagalli and G. Longoni, J. Organomet. Chem., 181 (1979) 233.

[73] J.C. Calabrese, L.F. Dahl, A. Cavalieri, P. Chini, G. Longoni and S. Martinengo, J. Am. Chem. Soc., 96 (1974) 2616.

[74] C.E. Briant, R.W.M. Wardle and D.M.P. Mingos, J. Organomet. Chem., 267 (1984) C49.

[75] D.M.P. Mingos and R.W.M. Wardle, J. Chem. Soc., Dalton Trans., (1986) 73.

[76] D.M.P. Mingos, P. Oster and D.J. Sherman, J. Organomet. Chem., 320 (1987) 257.

[77] D. Imhof, U. Burckhardt, K.-H. Dahmen, H. Rüegger, T. Gerfin and V. Gramlich, Inorg. Chem., 32 (1993) 5206.

[78] C.M. Hill, D.M.P. Mingos, H. Powell and M.J. Watson, J. Organomet. Chem., 441 (1992) 499.

[79] D.I. Gilmour and D.M.P. Mingos, J. Organomet. Chem., 302 (1986) 127.

[80] M. Arfelli, C. Battistoni, G. Mattogno and D.M.P. Mingos, J. Electron Spectrosc. Relat. Phenom., 49 (1989) 273.

[81] A.D. Burrows, H. Fleischer and D.M.P. Mingos, J. Organomet. Chem., 433 (1992) 311.

[82] A.D. Burrows, C.M. Hill and D.M.P. Mingos, J. Organomet. Chem., 456 (1993) 155.

[83] N.C. Payne, R. Ramachandran, G. Schoettel, J.J. Vittal and R.J. Puddephatt, Inorg. Chem., 30 (1991) 4048.

[84] A.D. Burrows, J.G. Jeffrey, J.C. Machell and D.M.P. Mingos, J. Organomet. Chem., 406 (1991) 399.

[85] J.J. Bour, R.P.F. Kanters, P.P.J. Schlebos, W. Bos, W.P. Bosman, H. Behm, P.T. Beurskens and J.J. Steggerda, J. Organomet. Chem., 329 (1987) 405.

[86] S. Bhaduri, K. Sharma, P.G. Jones and C.F. Erbrügger, J. Organomet. Chem., 326 (1987) C46.

[87] P. Braunstein, S. Freyburger and O. Bars, J. Organomet. Chem., 352 (1988) C29.

[88] O.J. Ezomo, D.M.P. Mingos and I.D. Williams, J. Chem. Soc., Chem. Commun., (1987) 924.

[89] A. Albinati, A. Moor, P.S. Pregosin and L.M. Venanzi, J. Am. Chem. Soc., 104 (1982) 7672.

[90] A.F. Wells, Structural Inorganic Chemistry, Clarendon, Oxford, 5th edn., 1984.

[91] A. Albinati, K.-H. Dahmen, F. Demartin, J.M. Forward, C.J. Longley, D.M.P. Mingos and L.M. Venanzi, Inorg. Chem., 31 (1992) 2223.

[92] G. Schoettel, J.J. Vittal and R.J. Puddephatt, J. Am. Chem. Soc., 112 (1990) 6400.

[93] A. Stockhammer, K.-H. Dahmen, T. Gerfin, L.M. Venanzi, V. Gramlich and W. Petter, Helv. Chim. Acta, 74 (1991) 989.

[94] A. Albinati, K.-H. Dahmen, A. Togni and L.M. Venanzi, Angew. Chem., Int. Edn. Engl., 24 (1985) 766.

[95] M.F. Hallam, D.M.P. Mingos, T. Adatia and M. McPartlin, J. Chem. Soc., Dalton Trans., (1988) 335.

[96] (a) Y. Yamamoto, H. Yamazaki and T. Sakurai, J. Am. Chem. Soc., 104 (1982) 2329.
(b) Y. Yamamoto and H. Yamazaki, J. Chem. Soc., Dalton Trans., (1989) 2161.

[97] T. Tanase, T. Horiuchi, Y. Yamamoto and K. Kobayashi, J. Organomet. Chem., 440 (1992) 1.

[98] E.G. Mednikov, N.K. Eremenko, V.V. Bashilov and V.I. Sokolov, Inorg. Chim. Acta, 76 (1983) L31.